



ELSEVIER

Available online at [www.sciencedirect.com](http://www.sciencedirect.com)

SCIENCE @ DIRECT®

Journal of volcanology  
and geothermal research

Journal of Volcanology and Geothermal Research 121 (2003) 155–193

[www.elsevier.com/locate/jvolgeores](http://www.elsevier.com/locate/jvolgeores)

## Deep submarine pyroclastic eruptions: theory and predicted landforms and deposits

James W. Head III<sup>a,\*</sup>, Lionel Wilson<sup>b</sup>

<sup>a</sup> *Department of Geological Sciences, Brown University, Providence, RI 02912, USA*

<sup>b</sup> *Environmental Science Department, Lancaster University, Lancaster LA1 4YQ, UK*

Received 31 October 2001; received in revised form 19 August 2002; accepted 19 August 2002

### Abstract

Submarine pyroclastic eruptions at depths greater than a few hundred meters are generally considered to be rare or absent because the pressure of the overlying water column is sufficient to suppress juvenile gas exsolution so that magmatic disruption and pyroclastic activity do not occur. Consideration of detailed models of the ascent and eruption of magma in a range of sea floor environments shows, however, that significant pyroclastic activity can occur even at depths in excess of 3000 m. In order to document and illustrate the full range of submarine eruption styles, we model several possible scenarios for the ascent and eruption of magma feeding submarine eruptions: (1) no gas exsolution; (2) gas exsolution but no magma disruption; (3) gas exsolution, magma disruption, and hawaiian-style fountaining; (4) volatile content builds up in the magma reservoir leading to hawaiian eruptions resulting from foam collapse; (5) magma volatile content insufficient to cause fragmentation normally but low rise speed results in strombolian activity; and (6) volatile content builds up in the top of a dike leading to vulcanian eruptions. We also examine the role of bulk-interaction steam explosivity and contact-surface steam explosivity as processes contributing to volcanoclastic formation in these environments. We concur with most earlier workers that for magma compositions typical of spreading centers and their vicinities, the most likely circumstance is the quiet effusion of magma with minor gas exsolution, and the production of somewhat vesicular pillow lavas or sheet flows, depending on effusion rate. The amounts by which magma would overshoot the vent in these types of eruptions would be insufficient to cause any magma disruption. The most likely mechanism of production of pyroclastic deposits in this environment is strombolian activity, due to the localized concentration of volatiles in magma that has a low rise rate; magmatic gas collects by bubble coalescence, and ascends in large isolated bubbles which disrupt the magma surface in the vent, producing localized blocks, bombs, and pyroclastic deposits. Another possible mode of occurrence of pyroclastic deposits results from vulcanian eruptions; these deposits, being characterized by the dominance of angular blocks of country rocks deposited in the vicinity of a crater, should be easily distinguishable from strombolian and hawaiian eruptions. However, we stress that a special case of the hawaiian eruption style is likely to occur in the submarine environment if magmatic gas buildup occurs in a magma reservoir by the upward drift of gas bubbles. In this case, a layer of foam will build up at the top of the reservoir in a sufficient concentration to exceed the volatile content necessary for disruption and hawaiian-style activity; the deposits and landforms are predicted to be somewhat different from those of a typical primary magmatic volatile-induced hawaiian eruption. Specifically, typical pyroclast sizes might be smaller; fountain heights may exceed those expected for the purely magmatic hawaiian case; cooling of

\* Corresponding author..

*E-mail addresses:* [james\\_head@brown.edu](mailto:james_head@brown.edu) (J.W. Head III), [l.wilson@lancaster.ac.uk](mailto:l.wilson@lancaster.ac.uk) (L. Wilson).

descending pyroclasts would be more efficient, leading to different types of proximal deposits; and runout distances for density flows would be greater, potentially leading to submarine pyroclastic deposits surrounding vents out to distances of tens of meters to a kilometer. In addition, flows emerging after the evacuation of the foam layer would tend to be very depleted in volatiles, and thus extremely poor in vesicles relative to typical flows associated with hawaiian-style eruptions in the primary magmatic gas case. We examine several cases of reported submarine volcanoclastic deposits found at depths as great as  $\sim 3000$  m and conclude that submarine hawaiian and strombolian eruptions are much more common than previously suspected at mid-ocean ridges. Furthermore, the latter stages of development of volcanic edifices (seamounts) formed in submarine environments are excellent candidates for a wide range of submarine pyroclastic activity due not just to the effects of decreasing water depth, but also to: (1) the presence of a summit magma reservoir, which favors the buildup of magmatic foams (enhancing hawaiian-style activity) and episodic dike emplacement (which favors strombolian-style eruptions); and (2) the common occurrence of alkalic basalts, the  $\text{CO}_2$  contents of which favor submarine explosive eruptions at depths greater than tholeiitic basalts. These models and predictions can be tested with future sampling and analysis programs and we provide a checklist of key observations to help distinguish among the eruption styles.

© 2002 Elsevier Science B.V. All rights reserved.

*Keywords:* submarine; basalt; eruptions; volcanoclastic; pyroclastic; hyaloclastite; hawaiian; strombolian

## 1. Introduction and background

Submarine volcanic eruptions occur at divergent plate boundaries (e.g. [Buck et al., 1998](#); [Macdonald, 1998](#); [Perfit and Chadwick, 1998](#); [Head et al., 1996](#)) and in intraplate areas, commonly building seamounts (e.g. [Keating et al., 1987](#); [Wessell and Lyons, 1997](#); [Schmidt and Schmincke, 2000](#)). In addition to effusive flows, submarine eruptions can produce pyroclastic deposits (e.g. composed of ‘solid fragments ejected from volcanoes’; [Cashman et al., 2000](#), p. 421) and hyaloclastic deposits (e.g. consisting of ‘fragments of volcanic glass formed by non-explosive shattering’; [Batiza and White, 2000](#), p. 361). [Rittmann \(1960\)](#) coined the term hyaloclastite for ash-sized basaltic particles produced in situ by breakage of pillow rinds during submarine extrusions. As pointed out by [Batiza and White \(2000\)](#), the term hyaloclastite is sometimes used broadly to include both explosively formed fragments as well as those particles produced in situ by breakage of pillow rinds and this term is commonly encountered in the literature where the difference cannot be or has not been ascertained. We follow the usage described above and in particular use the term pyroclastic to refer to solid fragments ejected from vents where we think that this can be determined, and hyaloclastite for ash-sized basaltic particles produced in situ by breakage of

pillow rinds during submarine extrusions where it is possible to determine this. If both types of deposits might be involved, or in case of uncertainty, we use the term volcanoclastic in order to minimize potential confusion.

A common assumption about submarine volcanic eruptions is that the pressure of the overlying water column is sufficient to suppress juvenile gas exsolution so that magmatic disruption and pyroclastic activity does not occur, except at sufficiently shallow depths (e.g. [Batiza and White, 2000](#)). For example, one of the most distinctive stages recognized in the evolution of seamounts is that related to the summits of edifices where sufficiently shallow water is reached that magmatic volatiles can be readily exsolved and accumulated, leading to magma disruption on discharge and thus to pyroclastic deposits. This depth is generally recognized to be about 200–1000 m and less, depending on magma composition and volatile content (e.g. [Kokelaar, 1986](#); [Bonatti and Harrison, 1988](#); [Gill et al., 1990](#); [Oshima et al., 1991](#); [Heikinian et al., 1991](#); [Binard et al., 1992](#); [Wright, 1996, 1999](#); [White, 1996](#); [Kano, 1998](#); [Fiske et al., 1998, 2001](#); [Hunns and McPhie, 1999](#)) and is referred to as the volatile fragmentation depth ([Fisher and Schmincke, 1984](#)).

Observations of seamount summits at various depths, however, have shown the presence of hy-

aloclastic and pyroclastic deposits ranging from scattered fragments deposited between pillow lavas to evidence for extensive deposits associated with eruptive vents. Lonsdale and Batiza (1980) reported the presence of extensive flows of volcanoclastics on the summits of four seamounts 800–1200 m above the flanks of the EPR interpreted to have formed in deep-water phreatomagmatic eruptions (see also Batiza et al., 1984). Smith and Batiza (1989) documented extensive volcanoclastic deposits at depths from 1240–2500 m on six additional seamounts near the EPR and located several vent areas (see also Maicher et al., 2000; Maicher and White, 2001). These deposits occur at a depth where pressure would seem to preclude the normal exsolution of magmatic volatiles to such a degree that they disrupt (e.g. Fisher and Schmincke, 1984), unless the magma volatile contents are unusually high (Devine and Sigurdsson, 1995; Dixon et al., 1997). There are a number of other possible mechanisms for producing pyroclastics and hyaloclastites, however (Kokelaar, 1986).

More recent exploration of the sea floor has revealed additional evidence for pyroclastic and hyaloclastic deposits at a range of depths and in several magmatic–tectonic environments. For example, Clague et al. (2002a) documented fragmental volcanoclastic deposits associated with volatile-rich alkalic magmas in the North Arch Volcanic Field, Hawai'i, at depths of 4.3 km. Lava bubble-wall fragments ('limu o Pele') interpreted to be formed by submarine hydrovolcanic explosions have been found on the summit of Lo'ihi Seamount at depths of 1.2 km (Clague et al., 2000). Similar 'limu o Pele' deposits have been found along the Gorda Ridge axis at 3.2 km depth, and interpreted to be evidence for strombolian activity (Clague et al., 2002c). Fouquet et al. (1998) found widespread volcanoclastic deposits at the Mid-Atlantic Ridge (MAR) axis at depths up to 1.7 km. Extensive recent exploration of the summit of Lo'ihi Seamount (Clague et al., 2002b) has shown evidence of phreatic, phreatomagmatic, hawaiian, and strombolian eruption products and activity at 1.2 km, including an 11-m thick section of layered volcanoclastic deposits. The Lo'ihi summit deposits include fine-

grained ash beds, spatter, bombs, 'limu o Pele', Pele's hair, and cored bombs (Clague et al., 2002b).

Thus, several major questions arise concerning the formation of pyroclastic and hyaloclastic deposits observed on the ocean floor and on seamounts (Fig. 1). What processes do these deposits represent in terms of mode of eruption, mechanisms of fragmentation, style of emplacement of deposits, and formation of landforms? What is the significance of these processes to the later stages of evolution in the overall development and shallowing of seamounts? The purpose of this paper is to address several aspects of these questions. We present a treatment of the theory of ascent and eruption of magma at a range of depths in the submarine environment, concentrating on processes which can lead to explosive activity. We make inferences about the most likely mechanisms and their sequence and relative importance. Finally, we compare these to several known occurrences and make predictions about the style of emplacement of deposits, and processes of formation of landforms, that can be tested by further observations.

## 2. Theory of the ascent and eruption of magma in the submarine environment

In the subaerial environment, magma ascending to shallow depths at speeds up to several meters per second typically undergoes gas exsolution in the upper several hundreds of meters of the dike, causing disruption and acceleration of magma through the conduit to produce lava fountaining (known as hawaiian-style activity) and a range of pyroclastic deposits is produced (Head and Wilson, 1987, 1989). In some cases, magma ascent is stalled or magma rise speeds relative to dike walls are less than bubble rise speeds through the magmatic liquid; in this case larger bubbles can overtake and coalesce with smaller ones to create small numbers of very large bubbles which burst at the surface of the magma column, causing strombolian-style eruptive behavior and deposits. In the deep submarine environment typical of the MAR or East Pacific Rise, pressures are high

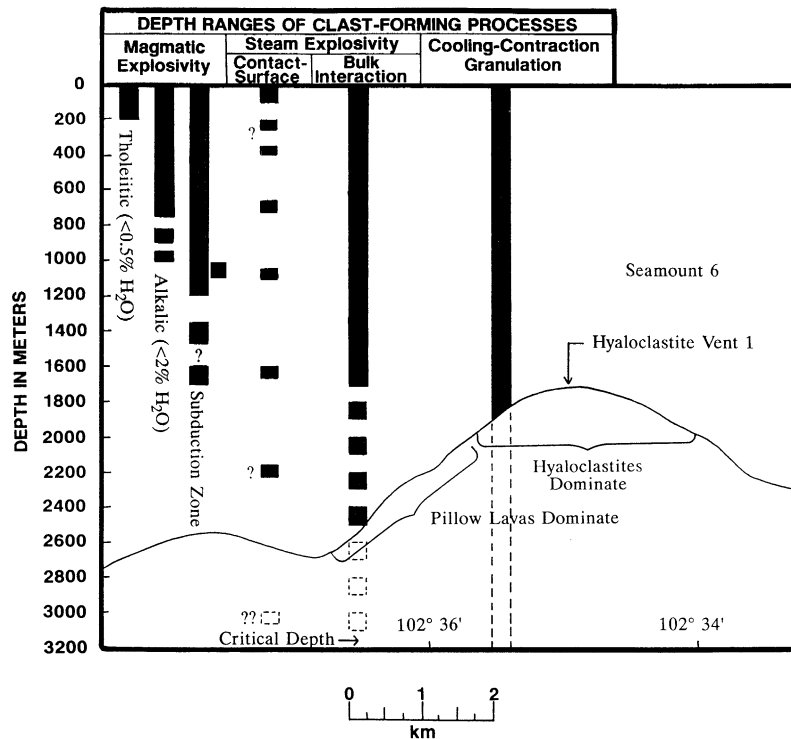


Fig. 1. General geologic setting, conditions, and environment of emplacement of magma and lavas in submarine seamounts. We take the specific size, shape and depth for the edifice Seamount 6, Eastern Pacific Ocean (data from Smith and Batiza, 1989), but the example is similar to conditions and observations on several seamounts (e.g. Smith and Batiza, 1989). Also shown are the depth ranges of various clast-forming processes on the sea floor (after Kokelaar, 1986).

enough to greatly reduce or completely inhibit gas exsolution so that continuous magma disruption and hawaiian-style pyroclastic deposits are normally precluded (Head et al., 1996).

However, there are circumstances which can lead to magma disruption and explosive activity at great water depths. In the following sections we explore these (Fig. 2), examining specifically: (1) eruption conditions when no magmatic gas is exsolved; (2) eruption conditions when magmas contain some gas bubbles but in a concentration too low to cause magma disruption; (3) the (high) levels of magma volatile content needed to ensure magma disruption and continuous explosive (hawaiian-style) activity even at high water pressures; (4) the (even higher) amounts of magmatic gas needed to allow gas exsolution and accumulation into a foam layer at the top of a magma reservoir which is then also released in a steady explosive discharge; and (5) the expected interactions be-

tween the overlying water and the explosively ejected gas and pyroclasts in hawaiian-style eruptions. Next, we (6) examine the circumstances in which slow magma rise speed can allow small numbers of gas bubbles to exsolve and then coalesce into a few large bubbles which cause intermittent explosive (strombolian) disruption of the magma surface when they reach the sea-floor vent, and finally (7) comment briefly on the conditions in which gas accumulation at the top of shallow dikes approaching close to the sea-floor could in principle lead to localised (vulcanian) explosions.

### 2.1. No gas exsolution

In this case (Fig. 2), there is no gas exsolution at all by the time the magma has risen to the level of the vent and decompressed to the ambient pressure level. This is unlikely unless magma

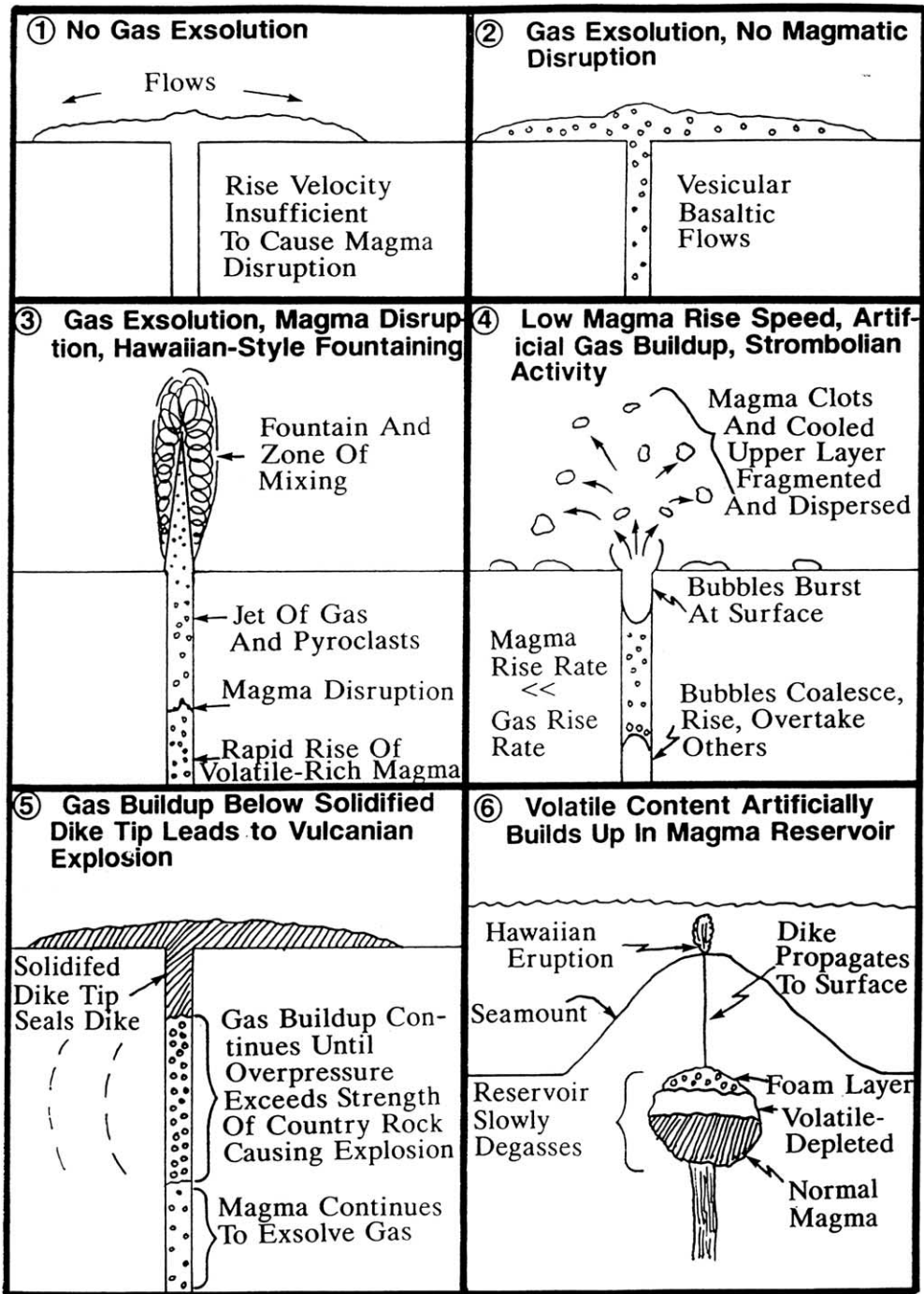


Fig. 2. Configuration of the ascent and eruption of magma in several possible submarine examples: (1) no gas exsolution; (2) gas exsolution but no magmatic disruption; (3) gas exsolution, magma disruption, and hawaiian-style fountaining; (4) volatile content builds up in the magma reservoir leading to foam formation; (5) magma volatile content insufficient to cause fragmentation normally but low rise speed results in strombolian activity; (6) volatile content builds up in the top of a dike leading to vulcanian eruptions.

CO<sub>2</sub> contents are extremely low, but if it is the case the consequences are that there will be virtually no fountaining. This case was treated for the subaerial environment by Head and Wilson (1987) for the Pu'u 'O'o vent on Kilauea volcano's East Rift zone. Using the observed magma volume flux to estimate the gas-free magma rise speed driven by magma buoyancy (0.4 m/s), they calculated that the gasless fountain height would be less than 1 cm and that, in order to approach average observed fountain heights of 200 m by discharge alone, the volume flux required would be 20 000 m<sup>3</sup>/s, more than 100 times the maximum flux observed. Are there additional non-volatile or non-buoyancy factors that could accelerate magma rise to produce fountain heights of 10–20 m, causing 'autodisruption' of the lava as suggested by Smith and Batiza (1989) to account for volcanoclastics on deep seamount summits? Analysis of a wide range of dike widths and reservoir conditions under sea floor environmental situations (Head et al., 1996) shows that even under the most extreme values of excess reservoir pressure, rise speeds will increase by less than a factor of 5, and fountains would not exceed a few tens of centimeters in height. Such a 'dynamic lava mound' fountaining process would not of itself lead to magma disruption, pyroclast formation, and dispersal.

### 2.2. Gas exsolution but no disruption

In this case (Fig. 2), some gas exsolves but the volume fraction of gas in bubbles stays small enough that magma disruption does not occur as long as the bubbles are uniformly distributed in the magma; a vesicular magma is erupted effusively from the vent. The critical gas volume fraction which must be exceeded to ensure magma disruption is commonly assumed to be ~75% (Sparks, 1978), but may range from 60 to 90% (Vergnolle and Jaupart, 1990) depending on the magma rheology and applied strain rate. Sampling of flows and vent-related lavas will provide quantitative information on the volatile content and amount of vesicularity. The eruption speed in this case is greater than that when no gas exsolves because there will be some expansion of the

gas between bubble nucleation and eruption, but is still likely to be less than 1 m/s (Head et al., 1996). Is contact-surface steam explosivity likely to contribute to hyaloclastite formation in either of these first two cases? On the basis of experiments (Wohletz and McQueen, 1984) impulse values of about 0.7 m/s are required to initiate fuel-coolant interactions leading to catastrophic disruption and formation of abundant hyaloclastites. This value is in excess of the highest effusion velocities calculated for sheet flows on the MAR (0.2–0.5 m/s) (Head et al., 1996), and so we do not expect magma disruption to occur.

### 2.3. Gas exsolution, disruption, hawaiian-style fountaining

In this case (Fig. 2), enough gas exsolves that the volume fraction of gas in bubbles exceeds the critical value cited in 2.2. Gas exsolution but no disruption, at some level below the vent (or in the extreme case just at the vent) and magma is disrupted. A hawaiian-style lava fountain eruption then takes place, though its appearance and products are expected to be different from those of a subaerial lava fountain eruption (Head and Wilson, 1987, 1989) because of the immediate interaction with the seawater (see 2.7. Volatile content builds up in the top of dike leading to vulcanian eruptions).

Magmas with volatile contents typical of those commonly seen in subaerial eruptions would not erupt explosively at depths greater than 200–1000 m (e.g. Kokelaar, 1986). Therefore, the analysis which follows is designed to establish what magma volatile contents would be needed in a steadily rising magma to ensure that a continuous stream of fragmented magma would be ejected from the vent in an underwater hawaiian-style or plinian-style jet. The requirement is that the exsolved magmatic volatile volume fraction reaches a critical value (which we assume to be ~75% for consistency with earlier work) by the time the magma has decompressed to the pressure level of the vent. Let this pressure be  $P_v$ , calculated as a function of depth below sea level using the acceleration due to gravity,  $g$ , = 9.8 m s<sup>-2</sup> and assuming a cold seawater density of 1026 kg m<sup>-3</sup>.

The partial volume fractions of the gas and liquid phases of the magma are given by the ratios of their masses and densities. Assume that in general finite amounts of both H<sub>2</sub>O (steam) and CO<sub>2</sub> have exsolved and let the volume fractions of these gases be  $V_s$  and  $V_c$ , respectively; the magmatic liquid volume fraction is  $V_m$ . If the amounts of the gases which have exsolved are  $n_s$  and  $n_c$ , in each case expressed as mass fractions of the total magma mass, we have:

$$V_s = (n_s Q T) / (m_s P_v) \quad (1)$$

$$V_c = (n_c Q T) / (m_c P_v) \quad (2)$$

$$V_m = (1 - n_s - n_c) / \rho_m \quad (3)$$

where  $Q$  is the universal gas constant (8314 kg kmol<sup>-1</sup>),  $T$  is the magma temperature, and  $m_s$  and  $m_c$  are the molecular weights of the steam and CO<sub>2</sub>, 18.02 and 44.00 kg kmol<sup>-1</sup>, respectively. We have assumed (an adequate approximation for the present purpose) that the gases obey the perfect gas law and are in thermal equilibrium with the magmatic liquid. We take as plausible values for mafic magmas  $T = 1255^\circ\text{C} = 1528\text{ K}$  and  $\rho_m = 2700\text{ kg/m}^3$ . If the gas is to occupy 75% of the total volume we require that  $(V_s + V_c) = 3 V_m$ , and so:

$$(n_s/m_s) + (n_c/m_c) = [(1 - n_s - n_c) P_v] / (Q T \rho_m) \quad (4)$$

Also, the definition of the bulk density  $\beta$  of the magma is  $(1/\beta) = (V_s + V_c + V_m)$ , and so in the general case we have:

$$(1/\beta) = [(Q T) / P_v] [(n_s/m_s) + (n_c/m_c)] + [(1 - n_s - n_c) / \rho_m] \quad (5)$$

In the special case of  $(V_s + V_c) = 3 V_m$  this becomes

$$(1/\beta) = [4(1 - n_s - n_c)] / \rho_m \quad (6)$$

Thus, for any chosen ocean depth, and hence pressure, we can find either the minimum value of  $n_s$  needed to ensure explosive disruption of the magma given a choice of the value of  $n_c$ , or the minimum value of  $n_c$  required given a choice of the value of  $n_s$ , together with the corresponding bulk density of the erupting fragmented magma.

To illustrate the extreme ranges of conditions we show in the first part of [Table 1](#) the values of  $n_s$  when  $n_c = 0$  and in the second part the values of  $n_c$  when  $n_s = 0$ . Also shown are the corresponding bulk magma densities  $\beta_s$  and  $\beta_c$  given by Eq. 6 and in addition the total amounts  $n_{st}$  and  $n_{ct}$  of the volatile phases which would have to be present in the magma prior to any gas exsolution, allowing for the solubilities  $n_{sd}$  and  $n_{cd}$  of these phases in basaltic melts given by:

$$n_{sd} = 6.8 \times 10^{-8} P_v^{0.7} \quad (7)$$

([Dixon, 1997](#)) and:

$$n_{cd} = 5.9 \times 10^{-12} P_v + 5.0 \times 10^{-6} \quad (8)$$

([Harris, 1981; Dixon, 1997](#)) where in each case the solubility is expressed as a weight fraction and the pressure  $P_v$  is expressed in Pa. These values of  $n_{st}$  and  $n_{ct}$  represent minimum requirements because they assume that no supersaturation of volatiles is needed to initiate gas bubble nucleation. However, significant supersaturations may be required at the pressures in submarine magma reservoirs ([Bottinga and Javoy, 1990](#)).

Vents at the summits of seamounts and mid-ocean ridges occur at water depths from several hundred meters to  $\sim 3500\text{ m}$ . [Table 1](#) shows that from  $\sim 0.8$  to  $\sim 5.3\text{ wt}\%$  water or alternatively  $\sim 2$ – $\sim 12\text{ wt}\%$  CO<sub>2</sub> would need to be exsolved to ensure continuous explosive activity at these depths (of course, if both volatiles are present, as is the case in practice, some critical combination of the two is required). On the basis of comparison of these values with typically mafic magma volatile contents (e.g. [Wallace and Anderson, 2000](#)), and with the most extreme volatile contents found in submarine basalts ( $\sim 1.4\text{ wt}\%$  CO<sub>2</sub> and  $0.54\text{ wt}\%$  H<sub>2</sub>O in a ‘popping rock’ from the MAR, [Javoy and Pineau, 1991; Pineau and Javoy, 1994](#);  $0.8$ – $1.0\text{ wt}\%$  CO<sub>2</sub> for similar MAR ‘popping rock’ samples, [Gerlach, 1991](#);  $0.68\text{ wt}\%$  H<sub>2</sub>O in a basalt possibly contaminated by seawater during a caldera collapse event at Lo’ihi, [Kent et al., 1999](#)) it is clear that the volatile contents required to produce hawaiian-style eruptions are very unlikely to be common (see also [Macdonald, 1967; Fornari et al., 1988; Dixon, 1997; Dixon and Clague, 2001; Dixon and Stolper,](#)

Table 1  
Values for a series of depths below the ocean surface  
(a) Gas phase is pure water

Depth (m)	$P$ (MPa)	$n_s$ (wt%)	$n_{st}$ (wt%)	$\rho_s$ (kg m <sup>-3</sup> )	$\beta_s$ (kg m <sup>-3</sup> )
500	5.13	0.802	1.139	7.27	680.3
1000	10.16	1.575	2.121	14.40	685.7
1500	15.18	2.337	3.061	21.54	691.2
2000	20.21	3.087	3.971	28.66	696.4
2500	25.24	3.825	4.858	35.80	701.9
3000	30.26	4.553	5.726	42.93	707.2
3500	35.29	5.359	6.665	50.06	713.2

(b) Gas phase is pure carbon dioxide

Depth (m)	$P$ (MPa)	$n_c$ (wt%)	$n_{ct}$ (wt%)	$\rho_c$ (kg m <sup>-3</sup> )	$\beta_c$ (kg m <sup>-3</sup> )
500	5.13	1.935	1.939	17.76	688.4
1000	10.16	3.761	3.767	35.17	701.4
1500	15.18	5.520	5.529	52.58	714.4
2000	20.21	7.216	7.228	70.00	727.5
2500	25.24	8.852	8.867	87.41	740.6
3000	30.26	10.432	10.450	104.82	753.6
3500	35.29	12.147	12.168	122.23	758.1

Values include the total ambient pressure,  $P$ , the minimum total mass fraction,  $n_s$  or  $n_c$ , of the volatile (pure water or pure carbon dioxide, respectively) that must be exsolved from a magma to allow explosive disruption of the magma to occur; the total amount of gas dissolved in the magma,  $n_{st}$  or  $n_{ct}$ , respectively, to permit this amount to exsolve; the density of the exsolved gas phase,  $\rho_s$  or  $\rho_c$ , respectively; and the bulk density,  $\beta_s$  or  $\beta_c$ , respectively, of the gas-pyroclast mixture that emerges through the vent.

1995; Dixon et al., 1991, 1995). However, Dixon et al. (1997) documented alkali basaltic/nephelinitic lavas erupted north of Hawai'i which contained 1.9 wt% H<sub>2</sub>O and 5.4% CO<sub>2</sub>; Table 1 shows that if these magmas had been erupted at depths shallower than about 1250 m, they would certainly have produced the submarine equivalents of hawaiian-style lava fountains even if only one or the other of the volatile components were present. Explosive activity at even greater depths is possible when both volatiles are taken into account.

We can demonstrate this, and also illustrate the likely eruption speeds in submarine hawaiian eruptions, by examining the eruption of the very volatile-rich magma documented by Dixon et al. (1997) at a range of water depths. First we establish the pressure at which such a magma would have a total exsolved gas volume fraction equal to 75%, thus causing magma fragmentation. This involves making an initial estimate of this pressure

and using Eqs. 7 and 8 to find the amounts of CO<sub>2</sub> and H<sub>2</sub>O dissolved in the magma; subtracting these values from the total volatile contents, 5.4 wt% CO<sub>2</sub> and 1.9 wt% H<sub>2</sub>O, gives the exsolved amounts of gas,  $n_c$  and  $n_s$ , respectively. These values are used in Eqs. 1–3, with the current pressure estimate being substituted for  $P_v$ , to find the partial volumes of CO<sub>2</sub>, H<sub>2</sub>O and magmatic liquid; the total gas volume fraction is then evaluated. If this is more or less than 75% the pressure is increased or decreased, respectively, and a new gas volume fraction is calculated. The process is repeated until enough values close to 75% are available to make accurate interpolation of the pressure corresponding to exactly 75% possible. This is found to be  $P_f = 21.557$  MPa, at which pressure  $n_c = 5.3867$  wt% CO<sub>2</sub> (i.e. virtually all of the 5.4 wt% available) and  $n_s = 0.9752$  wt% H<sub>2</sub>O (about half of the 1.9 wt% available) have exsolved. Eq. 6 shows that the bulk density  $\beta_m$  of the erupting gas-pyroclast mixture is 721 kg m<sup>-3</sup>.

The pressure of 21.56 MPa corresponds to an ocean depth of 2134 m, and so any putative explosive eruption must take place at a water depth shallower than this. We therefore select a series of depths  $d_v$  below the ocean surface at which a proposed vent is located, calculate the ambient pressure  $P_v$  at the vent for each depth, and then find the amount of energy,  $E$ , per unit mass of magma which is available to drive the eruption due to magmatic gas expansion between the magma fragmentation pressure  $P_f$  and the vent pressure  $P_v$ . This energy is given by (Wilson, 1980):

$$E = QT[(n_c/m_c) + (n_s/m_s)]\ln(P_f/P_v) + [(1-n_c-n_s)(P_f-P_v)/\rho_m] \tag{9}$$

The available energy  $E$  is shared between the potential energy needed to raise magma from the fragmentation level to the vent, the work done against friction with the walls of the dike through which the magma rises, and the kinetic energy of the accelerating mixture of gas and pyroclasts. Wilson and Head (1981) show that the work done against friction after the magma fragments is very small, and so we only need to evaluate the work done against gravity. If we assume that the pressure gradient in the erupting magma is close to the lithostatic gradient in the surrounding host rocks (arguments supporting this assumption are given by Wilson and Head, 1981), and take the host rock density to be  $\rho_h = 2700 \text{ kg m}^{-3}$  (to allow for a small amount of vesicularity in the ocean floor crust), then the vertical distance between the magma fragmentation depth and the sea-floor vent is  $d_f$  where  $(P_f - P_v) = (\rho_h g d_f)$  and the potential energy change per unit mass of magma is  $(g d_f) = [(P_f - P_v)/\rho_h]$ . If the average speed of gas and pyroclasts erupted through the vent is  $u_v$  the kinetic energy per unit mass is  $(0.5 u_v^2)$  and we have:

$$0.5u_v^2 = QT[(n_c/m_c) + (n_s/m_s)]\ln(P_f/P_v) + (P_f - P_v)\{[(1-n_c-n_s)/\rho_m] - (1/\rho_h)\} \tag{10}$$

Table 2 shows the values of  $d_f$ ,  $\beta_m$  and  $u_v$  for values of the depth to the vent,  $d_v$ , between zero (a subaerial eruption at sea-level) and the maximum possible water depth to allow an explosive

Table 2  
Submarine hawaiian-type lava fountain eruption conditions for a very volatile-rich magma containing 5.4 wt% CO<sub>2</sub> and 1.9 wt% H<sub>2</sub>O

$d_v$ (m)	$d_f$ (m)	$\beta_m$ (kg m <sup>-3</sup> )	$u_v$ (m/s)
0	811	3.5	556
250	716	92	340
500	621	181	275
750	526	269	230
1000	431	355	193
1250	338	440	161
1500	241	522	128
1750	147	601	94
2000	51	680	54
2100	13	711	27
2134	0	720	0

For various depths,  $d_v$ , of the vent below the ocean surface, values are given for: the depth below the vent at which magma is fragmented,  $d_f$ ; the bulk density of the erupting gas-pyroclast mixture,  $\beta_m$ ; and the mean eruption speed of gas and pyroclasts,  $u_v$ . The entry for  $d_v = 0$  corresponds to a subaerial eruption of this magma.

eruption for this magma, 2134 m. Note the dramatic increase in eruption speed as water depth becomes less than about 1000 m; in very shallow water or on land the eruption of a mafic magma with the volatile content used in this illustration would lead to a very violent, possibly plinian-style rather than hawaiian-style (Parfitt and Wilson, 1999), explosive eruption. Also note that all of the bulk magma densities  $\beta_m$  are less than the density of the seawater into which the magma erupts, so that the jet of volcanic ejecta is initially positively buoyant in the seawater.

As a second illustration of possible submarine hawaiian-style activity we have repeated the above analysis for the second most volatile rich submarine basalt mentioned earlier, that described by Javoy and Pineau (1991) and Pineau and Javoy (1994) with volatile contents of ~1.4 wt% CO<sub>2</sub> and 0.54 wt% H<sub>2</sub>O. Table 3 shows the results; the maximum depth for explosive activity is now very much less at ~489 m and the maximum eruption speed for eruptions in shallow water is ~250 m/s. Although less impressive than the previous example, this magma too would produce an extremely vigorous (~3000-m high) lava fountain if it erupted subaerially.

Table 3

Submarine hawaiian-type lava fountain eruption conditions for a moderately volatile-rich magma containing 1.4 wt% CO<sub>2</sub> and 0.54 wt% H<sub>2</sub>O

$d_v$ (m)	$d_f$ (m)	$\beta_m$ (kg m <sup>-3</sup> )	$u_v$ (m/s)
0	190	13	246
100	152	149	147
200	114	288	108
300	76	427	78
400	38	565	50
489	0	686	0

For various depths,  $d_v$ , of the vent below the ocean surface, values are given for: the depth below the vent at which magma is fragmented,  $d_f$ ; the bulk density of the erupting gas-pyroclast mixture,  $\beta_m$ ; and the mean eruption speed of gas and pyroclasts,  $u_v$ . The entry for  $d_v=0$  corresponds to a sub-aerial eruption of this magma.

The above analysis has been repeated for a wide range of permutations of initial magmatic CO<sub>2</sub> and H<sub>2</sub>O contents. Fig. 3 shows the maximum depth in the ocean at which a steady hawaiian-style explosive eruption can take place as a function of the H<sub>2</sub>O content for a series of fixed CO<sub>2</sub> contents. For each CO<sub>2</sub> content there is a

critical H<sub>2</sub>O content below which there is no further dependence on H<sub>2</sub>O; this is because in these cases magma fragmentation takes place solely due to the presence of CO<sub>2</sub> bubbles before any H<sub>2</sub>O exsolution has taken place.

We discuss the subsequent interactions between the products of hawaiian-style explosive eruptions and the overlying water in 2.5. [Submarine eruption plumes](#), after dealing in 2.4. [Volatile content builds up in the magma reservoir](#), with the other possible source of submarine hawaiian-style activity, gas accumulation in a magma reservoir.

#### 2.4. Volatile content builds up in the magma reservoir

It is theoretically possible to have circumstances in which explosive activity can be generated by a magma whose primary volatile content is insufficient to allow magma fragmentation to occur by the time the vent pressure is reached (Fig. 2). The requirement is that the magma must reside in a reservoir at a depth which is sufficiently shallow below the sea-floor to allow some volatile (mainly

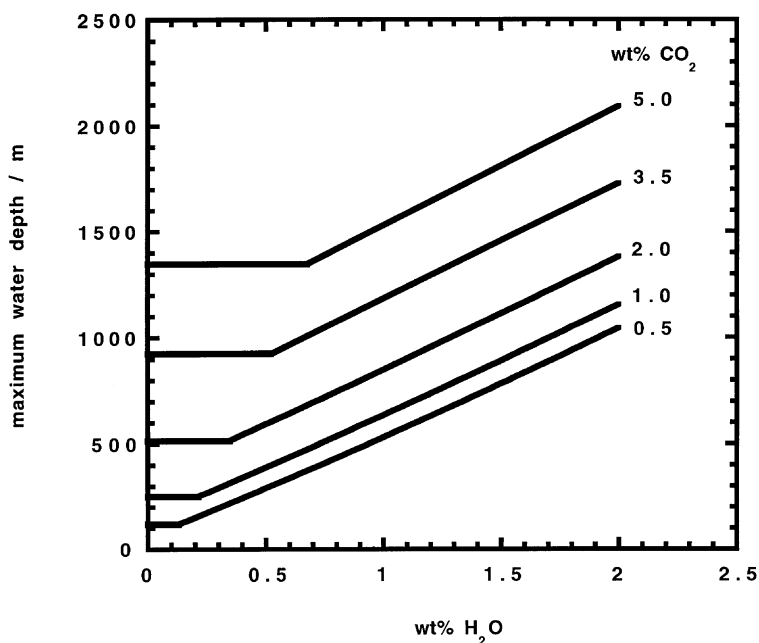


Fig. 3. The maximum depth in the ocean at which an eruption can be of the steady explosive hawaiian-style, shown as a function of the initial magmatic H<sub>2</sub>O content for a series of initial magmatic CO<sub>2</sub> contents. The depth ceases to depend on water content when magma fragmentation takes place solely due the presence of CO<sub>2</sub> bubbles before any H<sub>2</sub>O exsolution has taken place.

CO<sub>2</sub>) exsolution to occur over a finite range of depths below the roof of the reservoir (Bottinga and Javoy, 1990). Gas bubbles form and drift upwards to the roof where they accumulate into a foam layer in which the gas volume fraction is very high – greater than 90% is possible before the foam becomes unstable (Vergnolle and Jaupart, 1990). If this magmatic foam is subsequently erupted, it will be able to simulate the hawaiian-style eruption of a very gas-rich magma. This process has been proposed for some subaerial hawaiian eruptions (e.g. Vergnolle and Jaupart, 1990), though we note that it does not seem to be consistent with bubble growth rates in the ascending melts inferred from vesicle size distributions in the eruption products (Mangan et al., 1995). When all of the foam layer has been discharged, it may or may not be possible for the gas-depleted magma to be erupted after it – this will depend on the details of the magma density and magma reservoir pressure. However, it is not trivial to assume that magmatic foams can be retained in reservoirs in this way (in subaerial or submarine environments). When a foam layer exceeds a critical thickness, which is at most a few tens of meters (Vergnolle and Jaupart, 1990), the gas bubbles at the top of the foam will collapse and release gas into a continuous pocket which can escape into any cracks in the reservoir roof. Also, foam accumulation at the roof of a reservoir is itself a process encouraging the concentration of stress at the roof (Parfitt et al., 1993) and may lead to eruption initiation before very much accumulation has occurred.

If magmatic volatiles do exsolve and build up at the roof of a magma reservoir in this way (Fig. 2), it is necessary to find the minimum volatile content of the magma in the reservoir which will allow some gas exsolution to occur just below the roof. Consider a reservoir with its roof at a depth of 1000 m below the summit of a seamount which has its vent located at a water depth of 1500 m (Fig. 2). The pressure  $P_v$  at the vent is the sum of the overlying water weight plus the atmospheric pressure,  $(0.1 \text{ MPa} + [9.8 \text{ m s}^{-2} \times (1500 \text{ m} \times 1026 \text{ kg m}^{-3})]) = 15.18 \text{ MPa}$ . Using an edifice bulk density of  $\rho_e = 2700 \text{ kg m}^{-3}$  (to allow for a small amount of vesicularity in the eruption products

from which it is constructed), the pressure,  $P_r$ , at the level of the reservoir roof (which is the lowest pressure likely to exist in the magma in contact with the reservoir roof, see Parfitt et al., 1993) will be  $(P_v + [9.8 \text{ m s}^{-2} \times 1000 \text{ m} \times 2700 \text{ kg m}^{-3}]) = 41.64 \text{ MPa}$ . Table 1(a) shows that no H<sub>2</sub>O could exsolve at this pressure unless the water content of the magma was more than about 7.4 wt%, and so we assume that only CO<sub>2</sub> vapor is present. At a pressure of  $P_r = 41.64 \text{ MPa}$  the density  $\rho_{cr}$  of CO<sub>2</sub> with  $m_c = 44.00 \text{ kg kmol}^{-1}$  at magmatic temperature  $T = 1528 \text{ K}$  is  $\rho_{cr} = [(m_c P)/(QT)] = \sim 144.22 \text{ kg/m}^3$ . We require that a foam be formed which contains a large enough mass fraction of gas to allow magma fragmentation to occur when the foam decompresses to the pressure of a vent assumed to be at the 1500-m water depth of the summit of the seamount. We saw earlier that this corresponds to  $\sim 5.52 \text{ wt}\%$  CO<sub>2</sub>. If the volume fraction of CO<sub>2</sub> in the foam corresponding to this minimum mass fraction is  $X_{gmin}$  its mass fraction is  $(\rho_{cr} X_{gmin})$  whereas the mass fraction of the liquid magma with density  $\rho_m = 2700 \text{ kg/m}^3$  is  $(\rho_m \{1 - X_{gmin}\})$ . We therefore have:

$$n_c = (\rho_{cr} X_{gmin}) / (\rho_{cr} X_g + \rho_m \{1 - X_{gmin}\}) \quad (11)$$

and with  $n_c = 5.52 \text{ wt}\%$ , i.e. 0.0552, we find  $X_{gmin} = 0.5224$ . Thus, any foam that accumulates to the extent that the gas occupies at least 52.24% of the volume will lead to a hawaiian-style eruption when it erupts at the sea floor. Since foams with thicknesses of a few tens of meters can remain stable with gas volume fractions as high as at least  $\sim 90\%$  (Vergnolle and Jaupart, 1990), this is clearly a potential mechanism leading to submarine lava fountain eruptions at much greater depths than those illustrated earlier. The likely maximum volumes of magma that could be erupted in this way can be estimated by assuming that a 30-m thick foam layer with 80% gas volume fraction occupied an area of  $3 \text{ km}^2$ , approximately that of the roof of the summit magma chamber of Kilauea Caldera, Hawai'i (e.g. Ryan et al., 1983). The corresponding dense rock equivalent volume is then  $20 \times 10^6 \text{ m}^3$ , approximately ten times the amount released in a single eruptive

episode at Kilauea's Pu'u 'O'o vent (Wolfe et al., 1988).

The total amount of gas expansion which can occur to contribute significant energy to the eruption products is that which takes place between the level at which the magma is fragmented by gas bubble expansion and the vent level. In the example above, the build up of a foam in the reservoir to a volume fraction of 52.24% would just allow magma fragmentation at the vent but this would lead to essentially no acceleration due to gas expansion, and would yield only a very small eruption velocity. Interestingly, this situation maximizes the amount by which the gas bubbles in the magma can expand: decompression from the 242-MPa chamber roof pressure to the ~15-MPa vent pressure would lead to less than a 2-fold expansion of recently nucleated ~20- $\mu\text{m}$  diameter bubbles to at most ~40  $\mu\text{m}$ . If the foam builds up to a greater volume fraction, magma disruption occurs below the vent and although less pre-fragmentation bubble expansion occurs, more energy is available from subsequent gas expansion. We can estimate likely magma eruption speeds as follows. Assume that the gas volume fraction  $X_g$  in the foam at the roof of the magma reservoir is some value greater than the minimum value of  $X_{g\text{min}} = 0.5224$  found above. The  $\text{CO}_2$  gas mass fraction  $n_{\text{cr}}$  which corresponds to this volume fraction  $X_g$  is found from the equivalent of Eq. 11:

$$n_{\text{cr}} = (\rho_{\text{cr}} X_g) / (\rho_{\text{cr}} X_g + \rho_{\text{m}} \{1 - X_g\}) \quad (12)$$

Table 4 shows how  $n_{\text{cr}}$  varies if we let  $X_g$  increase from the minimum of  $X_{g\text{min}} = 0.5224$  to values as large as 0.9; gas mass fractions in excess of 0.3, i.e. 30 wt%, are possible. Also shown in Table 4 are the corresponding values of the bulk density  $\beta_{\text{m}}$  of the gas-pyroclast mixture which emerges through the vent when a foam with this large a gas content erupts at the vent pressure  $P_v = 15.18$  MPa. The values are found from Eq. 5 by substituting  $n_{\text{cr}}$  for  $n_c$  and setting  $n_s = 0$ , a reasonable approximation as Eq. 7 shows that no water is likely to be exsolved from magmas at this vent pressure unless they contain more than 0.7 wt%  $\text{H}_2\text{O}$ . All of the densities are substantially less than that of the overlying seawater.

We anticipate that gas concentrations as large as those found here will lead to very energetic submarine explosive eruptions. To estimate eruption speeds, we first need to know at what pressure  $P_d$  the magmatic foam will disrupt as it rises through the dike system from the level of the reservoir roof to the vent. We assume that, for foams with  $X_g$  initially less than 0.75, this will occur when the gas volume fraction has increased to 75%, i.e. when  $[(n_{\text{cr}} Q T) / (m_c P_d)] = 3 [(1 - n_{\text{cr}}) / 2700]$ , to give:

$$P_d = [2700 n_{\text{cr}} Q T] / [3 m_c (1 - n_{\text{cr}})] \quad (13)$$

We find the distance,  $d_d$ , below the vent at which the pressure  $P_d$  is reached by assuming, as in 2.3. Gas exsolution, disruption, hawaiian-style fountaining, that the pressure gradient in the erupting magma is close to the lithostatic gradient, so that  $(P_d - P_v) = \rho_e g d_d$ . In the case of foams with  $X_g$  initially greater than 0.75, magma disruption will presumably occur within the magma reservoir roof as the foam collapses so that  $P_d$  will be equal to  $P_r$ . We then find the mean eruption speed,  $u_v$ , of gas and pyroclasts at the vent by equating the kinetic energy per unit mass,  $(0.5 u_v^2)$ , to the energy due to gas expansion minus the

Table 4

The variation of the mass fraction,  $n_{\text{cr}}$ , of  $\text{CO}_2$  gas in a foam accumulating under the roof of a magma reservoir as a function of the volume fraction,  $X_g$ , of gas in the foam

$X_g$	$n_{\text{cr}}$ (wt%)	$P_d$ (MPa)	$d_d$ (m)	$\beta_{\text{m}}$ ( $\text{kg}/\text{m}^3$ )	$u_v$ (m/s)
0.5244	5.52	15.18	0	714	small
0.55	6.13	16.97	68	661	62
0.60	7.42	20.83	214	570	115
0.65	9.02	25.76	400	487	164
0.70	11.08	32.38	650	410	217
0.75	13.81	41.64	1000	339	279
0.80	17.60	41.64	1000	274	315
0.85	23.24	41.64	1000	213	362
0.90	32.47	41.64	1000	156	428

The reservoir is located at a depth of 1000 m below the summit of a submarine volcano and the summit vent is at a water depth of 1500 m. Also shown are the pressure,  $P_d$ , at which the foam disrupts into pyroclasts as it rises through a dike to the vent, the depth,  $d_d$ , below the vent at which this occurs, the bulk density  $\beta_{\text{m}}$  of the erupting gas-pyroclast mixture, and the velocity,  $u_v$ , with which the mixture erupts into the overlying water.

work done against gravity in rising the distance  $d_d$ ; the equivalent of Eq. 10 in 2.3. [Gas exsolution, disruption, hawaiian-style fountaining](#) becomes:

$$0.5u_v^2 = (QT/m_c)n_{cr}\ln(P_d/P_v) + (P_d - P_v)\{[(1 - n_{cr})/\rho_m] - (1/\rho_e)\} \quad (14)$$

Table 4 shows the values of  $P_d$ ,  $d_d$  and  $u_v$  resulting from foam gas volume fractions between the minimum of  $X_{gmin} = 0.5224$  and a likely upper limit of  $X_g = 0.9$ ; clearly eruption speeds of hawaiian-style lava fountains of more than 400 m/s are possible, even for a vent 1500 m below the surface. If foam build-up occurred in the magma reservoir of a volcanic edifice with its vent lying at shallower water depths then, as shown by the trends in Tables 2 and 3 for eruptions in which no concentration of volatiles occurs in this way, even higher eruption speeds would be possible. We now explore the likely interaction of both kinds of submarine lava fountains with the overlying water column.

### 2.5. Submarine eruption plumes

We saw in 2.3. [Gas exsolution, disruption, hawaiian-style fountaining](#), and 2.4. [Volatile content builds up in the magma reservoir](#), that continuous submarine explosive activity, in which a steady stream of fragmented magma is ejected from the vent into the overlying seawater column, can occur either when the magma is very rich in volatiles or when volatiles accumulate in a foam layer at the roof of a magma reservoir. We now treat the consequences of the interaction between a steadily erupting gas-pyroclast jet and the overlying water as follows. First, as illustrated in Fig. 4, assume that a fissure vent of width  $W$  and along-strike length  $S$  is at a depth where the pressure is  $P$  and is erupting a steady jet of disrupted magma consisting of clots of liquid with unvesiculated density  $\rho_m$  entrained in a mixture of gaseous water and carbon dioxide, all the components being at the same temperature  $T$ . In keeping with the examples shown in Tables 2 and 3, the bulk density of the erupting mixture is  $\beta_m$  and the

mean velocity of the jet is  $u_v$ . The mass flux of magma emerging from the vent is  $M$  where:

$$M_0 = \beta_m u_v WS \quad (15)$$

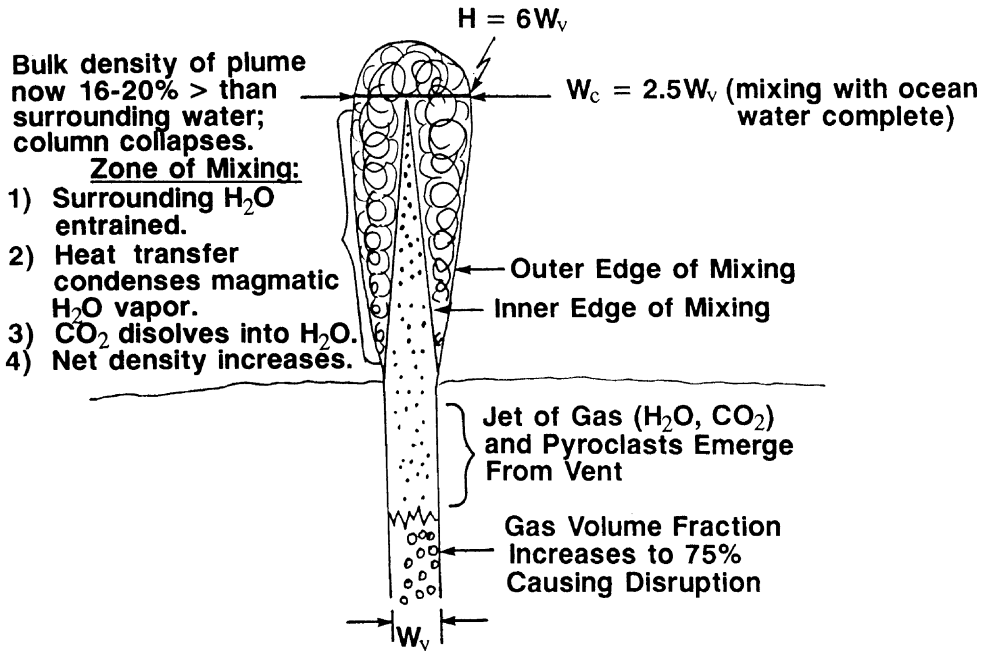
and the momentum flux is  $Z_0$  where:

$$Z_0 = \beta_m u_v^2 WS. \quad (16)$$

The momentum flux will be conserved as mixing with the surrounding water takes place, but the total mass flux will increase as ocean water is added to the widening plume. We therefore need to evaluate the mass flux immediately after the erupting jet has completed the first phase of its interaction with the surrounding seawater. We assume that the mixing takes place under conditions similar to those described by Prandtl (1949) for the turbulent interaction of a jet of fluid entraining a surrounding fluid having a similar density. This is not unreasonable given the densities found above for volcanic fluids just able to erupt explosively on the ocean floor. The volcanic jet mixes with the surrounding water in a fixed geometric pattern (Fig. 4) so that the inner edge of the zone of mixing extends from the edge of the vent to the center-line of the jet in the time it takes the mixture to rise to a height  $h_m = 6W$ , where  $W$  is the vent width. At the same time the outer edge of the mixing zone extends away from the edge of the vent by an amount  $(h_m/8)$  on either side of the jet, so that the full width of the widening jet just after it is fully mixed with the surrounding water is  $[W + 2(h_m/8)] = [W + 2(6W/8)] = (5/2)W$ . Given the range of dike widths, up to  $\sim 2$  m, estimated for submarine rise crest eruption (Head et al., 1996), we infer that  $h_m$  is typically  $\sim 12$  m and the width of the jet after mixing is  $\sim 5$  m. We assume (and will justify retrospectively) that during this mixing process two things happen: first, enough heat is transferred to the entrained water that all of the magmatic water vapor condenses into liquid water with density  $\rho_w$  and, second, that all of the carbon dioxide dissolves into the water. These assumptions can be used to calculate the resulting bulk density of the mixture as follows.

Consider a reference volume  $V$  located immedi-

**A** SUBMARINE HAWAIIAN ERUPTION BEHAVIOR



**B**

SUBMARINE HAWAIIAN ERUPTION PLUME

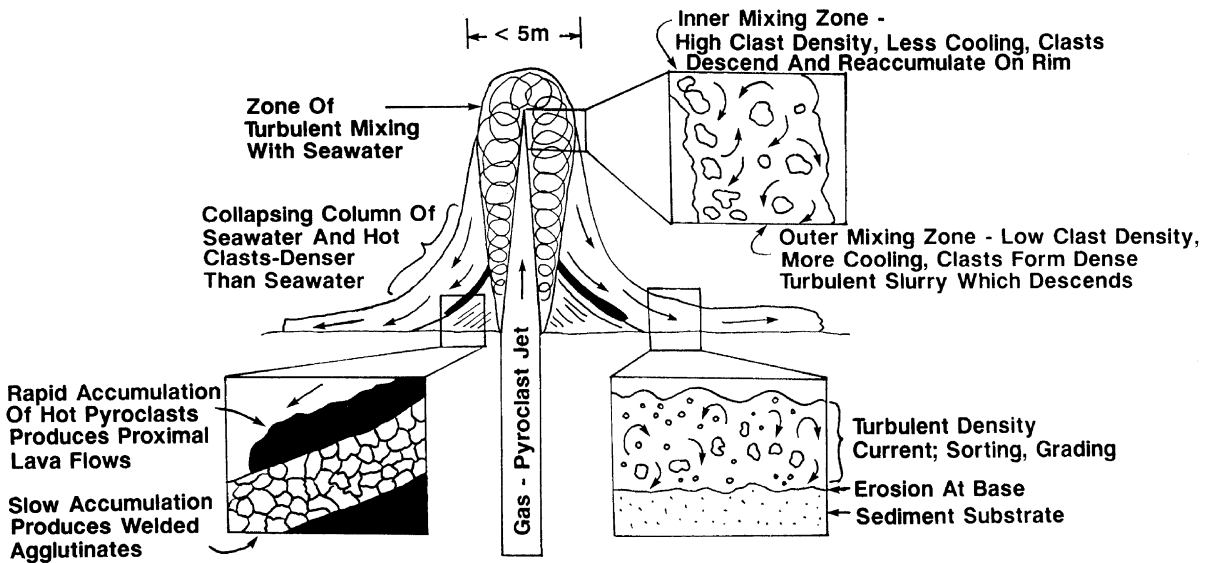


Fig. 4. Submarine hawaiian eruption model developed in this analysis. (A) Formation and emergence of gas/pyroclast jet and development of the zone of mixing. (B) Evolution and collapse of the zone of mixing to form flows, welded agglutinates, and density currents.

ately above the vent so that  $V$  is proportional to the vent width  $W$ . If the bulk density of the erupting fluid is  $\beta_m$  then the total mass within the volume  $V$  is  $(V \beta_m)$ . The mass of volcanic water vapor must therefore be  $(n_s V \beta_m)$  and this occupies a volume  $(n_s V \beta_m / \rho_s)$ . Similarly, the mass of  $\text{CO}_2$  is  $(n_c V \beta_m)$  in a volume  $(n_c V \beta_m / \rho_c)$  and the mass of rock is  $[(1-n_s-n_c) V \beta_m]$  in a volume  $[(1-n_s-n_c) V \beta_m / \rho_m]$ . Now consider the conditions after mixing with the ocean water is complete and the edges of the jet have expanded to the width  $(5/2) W$ . The reference volume has enlarged to  $(5/2) V$ , but within it the volume of rock is still  $[(1-n_s-n_c) V \beta_m / \rho_m]$ . Because the volcanic water has condensed, its volume is now  $(n_s V \beta_m / \rho_w)$  and the volume of the dissolved carbon dioxide is of course zero. So the volume of ocean water that has been entrained must be  $\{(5/2) V - [(1-n_s-n_c) V \beta_m / \rho_m] - (n_s V \beta_m / \rho_w)\}$  and its mass must therefore be  $\{[(5/2) - [(1-n_s-n_c) \beta_m / \rho_m] - (n_s \beta_m / \rho_w)] \{V \rho_w\}\}$ . The total mass within the volume  $(5/2) V$  consists of this entrained water mass plus the original masses of rock, volcanic water vapor and  $\text{CO}_2$ , i.e.  $[(1-n_s-n_c) V \beta_m]$ ,  $(n_s V \beta_m)$  and  $(n_c V \beta_m)$ , respectively. The new bulk density,  $\beta$ , is therefore this total mass divided by the new volume and, after a little simplification, is found to be:

$$\beta = \rho_w + (2\beta_m/5)\{1-n_s-[(1-n_s-n_c)(\rho_w/\rho_m)]\} \tag{17}$$

Given this value for the bulk density of the mixture of volcanic materials and seawater we can evaluate the velocity of the mixture. The momentum flux from the vent,  $Z_0$ , given by Eq. 16, must be equal (since momentum is conserved) to the momentum flux  $Z$  in the mixed, expanded plume, given by:

$$Z = \beta u^2 (5/2) WS \tag{18}$$

and hence:

$$u/u_v = [(0.4\beta_m)/\beta]^{1/2} \tag{19}$$

The mean temperature of the mixture can be found by equating the enthalpies of the components before and after mixing has taken place and can be represented by:

$$[(1-n_s-n_c)V\beta_m]c_r(T-T_e) + (n_sV\beta_m)h(T-T_e) + (n_cV\beta_m)c_c(T-T_e) = \{[(5/2)-((1-n_s-n_c)\beta_m/\rho_m)-(n_s\beta_m/\rho_w)]\{V\rho_w\}\}h(T_e-273.15) \tag{20}$$

where  $T$  is the eruption temperature of the magma as before,  $T_e$  is the final equilibrium temperature of the mixture and it has been assumed that the ocean water is just above the freezing point at 273.15 K.  $c_r$  and  $c_c$  are the average specific heats at constant pressure over the  $\sim 273$ – $1528$  K temperature range of interest of basaltic rock and carbon dioxide,  $\sim 1200$  and  $\sim 900$  J  $\text{kg}^{-1}$ , respectively, and  $h(T_x-T_y)$  is the specific enthalpy change of water between any temperatures  $T_x$  and  $T_y$ , obtained from UKCPS (1970). Use of the enthalpy eliminates the need to keep track of the temperature variation of the specific heat of water and, when the pressure is less than the  $\sim 22$  MPa critical pressure, to include the latent heat.

For each of the eruptions illustrated in 2.4. Volatile content builds up in the magma reservoir, and 2.5. Submarine eruption plumes, Table 5 shows the results of mixing with seawater. Table 5(a) deals with the eruption of the very volatile-rich magma, Table 5(b) with the moderately volatile-rich magma, and Table 5(c) with the case of foam accumulation in a reservoir. For each water depth of the vent, the magma density and eruption speed in the vent from Tables 2–4 are repeated for ease of comparison with the mixture density and upward speed after mixing has taken place. A number of interesting features are seen in Table 5. First, the velocity,  $u$ , after mixing is typically no more than one third of that before mixing. Second, whereas in all cases the bulk density of the jet of disrupted magma emerging from the vent is at least four times smaller than the density of the surrounding water before mixing takes place, after mixing is complete the bulk density of the jet is always greater than that of the surrounding water, typically by 10–20% (except for the shallowest eruptions where the density difference can become quite small). This finding differs from the qualitative expectation of Cashman and Fiske (1991) that the mixtures should be less

Table 5

Illustrations of the consequences of steadily erupted gas–pyroclast jets interacting with seawater. Part (a) deals with the eruption of the very volatile-rich magma shown in Table 2, part (b) with the moderately volatile-rich magma shown in Table 3, and part (c) with the case of foam accumulation in a reservoir shown in Table 4.

(a) Very volatile-rich magma contains 5.4 wt% CO<sub>2</sub> and 1.9 wt% H<sub>2</sub>O

$d_v$ (m)	Before mixing		After mixing				
	$\beta_m$ (kg m <sup>-3</sup> )	$u_v$ (m/s)	$\beta$ (kg m <sup>-3</sup> )	$u$ (m/s)	$h_f$ (m)	$T_e$ (°C)	BP (°C)
0	3.5	556	n/a	n/a	n/a	n/a	(n/a)
50	21	450	1031	41	84	5	(159)
250	92	340	1049	64	206	13	(226)
500	181	275	1072	71	260	26	(265)
750	269	230	1094	72	265	39	(291)
1000	355	193	1116	69	242	52	(312)
1250	440	161	1137	63	201	63	(328)
1500	522	128	1158	54	151	76	(343)
1750	601	94	1179	43	94	87	(355)
2000	680	54	1199	26	33	98	(366)
2100	711	27	1206	13	9	104	(370)
2134	720	small	n/a	small	small	105	(372)

(b) Moderately volatile-rich magma contains 1.4 wt% CO<sub>2</sub> and 0.54 wt% H<sub>2</sub>O

0	13	246	n/a	n/a	n/a	n/a	(n/a)
50	80	177	1046	31.0	49.0	11	(159)
100	149	147	1063	34.7	61.4	21	(184)
200	288	108	1098	34.9	62.1	41	(212)
300	427	78	1133	30.4	47.0	61	(236)
400	565	50	1167	22.1	24.9	82	(252)
489	686	small	n/a	small	small	99	(263)

(c) Foam accumulates under the roof of a magma reservoir

$X_{gmin}$ (m)	Before mixing		After mixing				
	$\beta_m$ (kg m <sup>-3</sup> )	$u_v$ (m/s)	$\beta$ (kg m <sup>-3</sup> )	$u$ (m/s)	$h_f$ (m)	$T_e$ (°C)	BP (°C)
0.5244	714	small	n/a	small	small	n/a	(n/a)
0.55	661	60	1196	28	40	90	(343)
0.60	570	106	1174	47	111	81	(343)
0.65	487	166	1154	68	237	69	(343)
0.70	410	220	1135	84	357	57	(343)
0.75	339	284	1117	99	500	47	(343)
0.80	274	320	1101	101	519	38	(343)
0.85	213	368	1086	103	541	29	(343)
0.90	156	435	1072	105	560	20	(343)

For each water depth of the vent,  $d_v$ , in parts (a) and (b), and for each gas volume fraction in part (c), the magma density  $\beta_m$  and eruption speed  $u_v$  in the vent are repeated from Tables 2–4 for ease of comparison with the mixture density  $\beta$  and upward speed  $u$  after mixing has taken place.  $h_f$  is the height to which the fountain rises over the vent and  $T_e$  is the equilibrium temperature after complete mixing between the erupted jet and the entrained seawater. The final column gives the water boiling point, BP, at the pressure implied by the depth  $d_v$  for comparison with  $T_e$ .

dense than the surrounding ocean water: our quantitative analysis shows that the influence of the loading of the entrained pyroclasts is greater than they anticipated. Third, the thermal calculation shows that the temperature after mixing is

always much less than the boiling point at the ambient pressure. Thus the earlier assertion that all of the volcanic steam condenses during the initial phase of mixing with the surrounding water is always entirely justified. Finally, we give in Ta-

ble 5 the values of the maximum height  $h_f$ , equal to  $[u^2/(2g)]$ , to which the materials in the jet could rise above the vent if there were no further significant interaction with the surrounding seawater. These are seen to range from tens of meters in the case of the moderately volatile-rich magma, Table 5(b), to hundreds of meters in the case of the very volatile-rich magma, Table 5(a), and the foam, Table 5(c). In Table 5(c), where the vent is at 1500 m depth, the volcanic materials do not reach depths shallower than 950 m despite the high eruption speeds. However, in the case of a vent at 50 m depth in Table 5(b), materials do almost reach the surface (nominally failing to do so by 1 m); and in the case of a vent at 50 m depth in the more volatile-rich case in Table 5(a), the 84-m rise distance implies that the mixture of pyroclasts and entrained water should overshoot the ocean surface by  $\sim 34$  m.

In fact, the motion of the pyroclasts and entrained seawater after mixing is complete just above the vent is much more complex than implied by the calculation of  $h_f$  described above. The conditions are similar to those in subaerial eruptions in which not enough atmosphere is entrained into the jet of volcanic materials emerging from a vent to ensure convective rise of the resulting plume and are consistent with the scenario described by Kokelaar and Busby (1992) to explain the deposits of a more silicic submarine explosive eruption. In general the mixture collapses back to the ocean floor as a density current from a height of order  $h_f$  at a speed similar to  $u$ , and the entire structure resembles a vertical fountain over the vent. The internal motions of such a system are complex, particularly because the jet rising from the vent is now entraining not seawater but the descending part of the fountain which will be denser than seawater by an amount similar to that found in the above mixing calculation. The treatment of subaerial volcanic fountains by Wilson and Heslop (1990) shows that the dynamic pressure exerted by the falling material can cause the pressure in the vent in such systems to rise well above the ambient pressure, reducing the velocity of the fountain at its base (and hence its rise height) because less gas expansion occurs. However, this phenomenon is very much less pro-

nounced in the submarine environment. The dynamic pressure exerted by the falling material is  $[(1/2) \beta u^2]$ , and using the values in Table 5 this is only a significant fraction of the ambient water pressure at the vent depth for vents shallower than  $\sim 50$  m.

More important is the uncertainty related to the decoupling of the motions of the pyroclasts of various sizes from that of the entrained water (e.g. Cashman and Fiske, 1991; Kokelaar and Busby, 1992; Davis and Clague, 1998; White, 2000). All of the clasts will have a finite terminal velocity in the water and will therefore lag behind the upward water speed by this amount. The terminal velocities of 1-m, 10-cm, 1-cm and 1-mm sized particles will be of order 3, 1, 0.3 and 0.1 m/s, respectively; these values assume clast densities of  $\sim 1500 \text{ kg m}^{-3}$  (implying significant vesicularity) and include due allowance for the buoyancy of the clasts in the water (Cashman and Fiske, 1991), giving them an effective density of  $\sim 500 \text{ kg m}^{-3}$ , but they will not be as much as a factor of 2 greater even if there is no vesicularity. Thus, only very large magma clots emerging through the vent will decouple significantly from the water motion near the vent in explosive submarine eruptions. Given the range of speeds after mixing in Table 5(a)–(c), say 30–100 m/s, the timescales  $[(2u)/g]$  for clasts to pass completely through the fountain over the vent will be 3–10 s, and the thicknesses of the chilled skins on any clasts in direct contact with seawater will be up to  $\sim (\kappa t_f)^{1/2} = \sim 3 \text{ mm}$ , where  $\kappa$  is the thermal diffusivity of rock,  $\sim 10^{-6} \text{ m}^2/\text{s}$ . Thus, in general (though see also the discussion below) cm-sized and smaller pyroclasts will undergo significant heat loss, whereas larger magma clots will reach the surface with a chilled skin surrounding a largely hot interior.

The primary size frequency distribution of fragments resulting from submarine explosive eruptions is poorly known. Also poorly understood are the auxiliary processes (discussed in a following section) that might operate on the pyroclasts in this environment, such as the influence of contact-surface steam explosivity on the pyroclasts in the mixing zone (Kokelaar, 1986). For example, as more clasts come into contact with seawater in

the outer parts of the descending column (Fig. 4), water is vaporized, and the clasts cool and may shatter, potentially leading to fuel–coolant interactions. Despite these uncertainties, the general fate of pyroclasts in this environment is clear. The high density of the surrounding water column, relative to the subaerial environment, means that particles are decelerated dramatically in the narrow mixing zone and eruption jet dispersal is inhibited relative to the subaerial environment. Thus, most pyroclasts will begin to fall in the immediate vicinity of the vent (within a few meters radius) due to the negative buoyancy of the mixed zone.

Particles may have several fates, depending on their position in the jet and zone of mixing (Fig. 4). In the inner part of the column, where cooling is least, clasts are hottest and clast number density is highest, the descending clasts may reaccumulate and coalesce to form a lava flow or a lava pond feeding a flow. Toward the outer part of the column, clast number density is less, more cooling has occurred, the mixing zone is negatively buoyant, and column collapse will result in density currents descending down the margins of the column, reaching the surface in the vicinity of the vent, and expanding out into the surrounding areas at initial speeds of order at least 30–100 m/s (e.g. Table 5(b),(c)) as potentially erosive, pyroclast-charged density flows. The runout distances of such flows will be controlled much more by mixing with the overlying water than by basal friction. If the geometry of the mixing process is the same as that in the vertical part of the plume we might expect runout distances of order twice the plume height, i.e.  $\sim 1$  km for foam driven hawaiian plumes. In the outermost parts of the collapsing column, extensive mixing with water may elutriate many (relatively small) clast sizes into the submarine equivalent of a subaerial cognimbrite eruption cloud (Fig. 4; Kokelaar and Busby, 1992). The relatively high effusion rates associated with hawaiian-type eruptions would lead to the prediction that any lava flows associated with these events would be characterized by lobate sheets, rather than pillows (e.g. Head et al., 1996; Gregg and Fink, 1995).

In summary, submarine hawaiian eruptions will

produce low, narrow eruption jets, which will quickly collapse to produce proximal accumulations of hot coalescing pyroclasts within a few meters of the vent and cooler, less clast-rich density flows descending from the distal parts of the column and spreading radially away from the vent for distances of the order of the height of the column (relative to the subaerial case, density flows are subjected to additional drag at their upper surfaces by the submarine medium). Landforms anticipated from these eruptions (Fig. 4) might include cones surrounding the vent with rim crests within a few meters of the vent (much closer than in the subaerial case), possible lava ponds within the cone, and an apron of pyroclastic deposits surrounding the vent. The cone and the flanking deposits should consist of interlayers of pyroclastic flows and lava flows with sheet flow morphology, rather than pillow lava morphology dominating. At greater radial distances from the vent (Fig. 4), one would predict that flows and layers of agglutinated pyroclasts would dominate proximally in the cone, giving way to bedded pyroclastics and interlayered lava flows distally.

Explosive eruptions driven by foam layer collapse should produce generally similar deposits and landforms to those from normal magmatic volatile-induced hawaiian eruptions but with some systematic differences. Thus, typical pyroclast sizes might be smaller (due to the greater amount of gas bubble expansion), and the pyroclasts themselves may be dominated by shattered bubble walls forming ‘limu o Pele’. Cooling of descending pyroclasts in the outer parts of the collapsing fountains would be more efficient because fountain heights would exceed those expected for purely magmatic cases, leading to different types of proximal deposits. Runout distances for density flows would also be greater, potentially leading to surrounding pyroclastic deposits in the tens to hundreds of meters range. In general, the volatile buildup at the top of the reservoir would leave a complementary volatile-depleted magma below. Thus, after the volatile-rich layer was discharged during the hawaiian-style eruption event, it could be followed by a very volatile-depleted effusive phase, and vesicle-poor lavas overlying pyroclastic-rich cones might there-

fore be a distinctive signature of this eruption setting. However, Blake (1981) has shown that typically less than 1% of the total volume of the melt in a reservoir leaves the reservoir in individual overpressurization-induced diking events. Thus, it is entirely possible that only the volatile rich foam layer might be erupted.

### 2.6. No normal fragmentation, but low rise speed causes strombolian activity

Sufficiently volatile-poor magmas cannot erupt explosively as long as the bubbles are uniformly distributed in the magma; however, explosive activity may occur if the magma rise speed in the dike/conduit feeding the vent is so slow that there is time for large, early-nucleated bubbles to overtake smaller, later-nucleated bubbles in a runaway bubble coalescence process (Figs. 2 and 5A). The intermittent emergence of the resulting giant bubbles through the lava at the vent drives strombolian explosions. Since this mode of eruption requires a relatively low magma rise speed in the dike, it is most likely to be associated with low effusion rate eruptions. If a lava lake is present around the vent (Fig. 5B), the intermittent large bubbles burst through its surface and throw up magma clots whose size and shape (and launch speed) are dictated by the radius of the bubble, its arrival speed at the surface (larger bubbles travel faster) and the degree of cooling and hence non-Newtonian behavior of the lake surface (the higher the eruption rate the more rapidly the lake overflows to feed flows and the hotter its surface stays, on average, leading to easier deformation and smaller pyroclast sizes). If no lava lake is present over the vent, the large bubbles rising up the dike simply blow off the magma just ahead of them (Fig. 5A). In this case the magma is inevitably hotter than if it had been sitting in a lava lake. The pyroclast sizes to be expected in this case are hard to predict. Because strombolian activity is most likely to occur in magmas with low exsolved gas contents, this implies that the magma between the large bubbles will contain relatively small numbers of small gas bubbles and so will certainly not have any strong tendency to disrupt further into small fragments; in the extreme case

the largest magma clots ejected might have their longest axes comparable to the width of the dike.

We can explore the ranges of eruption conditions that give rise to strombolian activity in a magma that has too low a volatile content to allow hawaiian-style activity to occur. For any chosen magma viscosity and total volatile content there is a critical magma rise speed below which there will be extensive bubble coalescence and strombolian activity will be unavoidable. A computer program to simulate coalescence numerically was developed by Wilson and Head (1981) and Parfitt and Wilson (1995). We have used this program to find the maximum magma rise speeds,  $u_s$ , allowing strombolian activity when the volatile involved is CO<sub>2</sub> and the eruptive vent is at least 1500 m below sea level. These rise speeds have implications for the widths of the dikes through which the eruptions are occurring. A magma with a given viscosity  $\eta$  will have a rise speed  $u_s$  which is a function of the dike width  $W_s$  and the pressure gradient  $dP/dz$  driving the motion (Wilson and Head, 1981) such that in laminar flow (which can be shown to be the relevant condition for all of the cases above by retrospectively calculating the Reynolds number of the motion):

$$u_s = (W_s^2 dP/dz)/(12\eta) \quad (21)$$

For submarine eruptions Head et al. (1996) show that a plausible pressure gradient is  $dP/dz = 2000$  Pa/m, and with this value we find the maximum dike widths allowing strombolian activity to occur shown in Table 6. The values, always significantly less than 1 m, ensure that conductive cooling and solidification of the dike will be relatively rapid (Wilson and Head, 1988; Bruce and Huppert, 1989; Head et al., 1996) and that, in the submarine environment, strombolian eruption events will typically last on the order of hours, rather than days.

Using these calculations, we can now estimate the characteristics and evolution of the eruption process and make predictions about the resulting deposits and landforms. Initial stages of a strombolian eruption might be characterized by dike emplacement and extrusion of lavas at very low effusion rates, leading to production of short

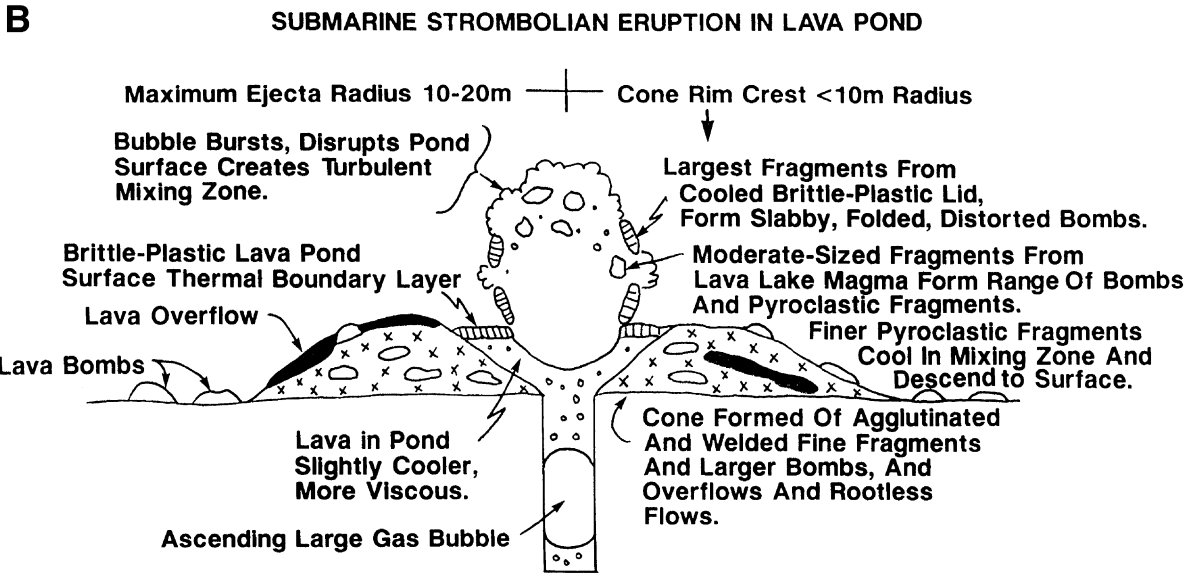
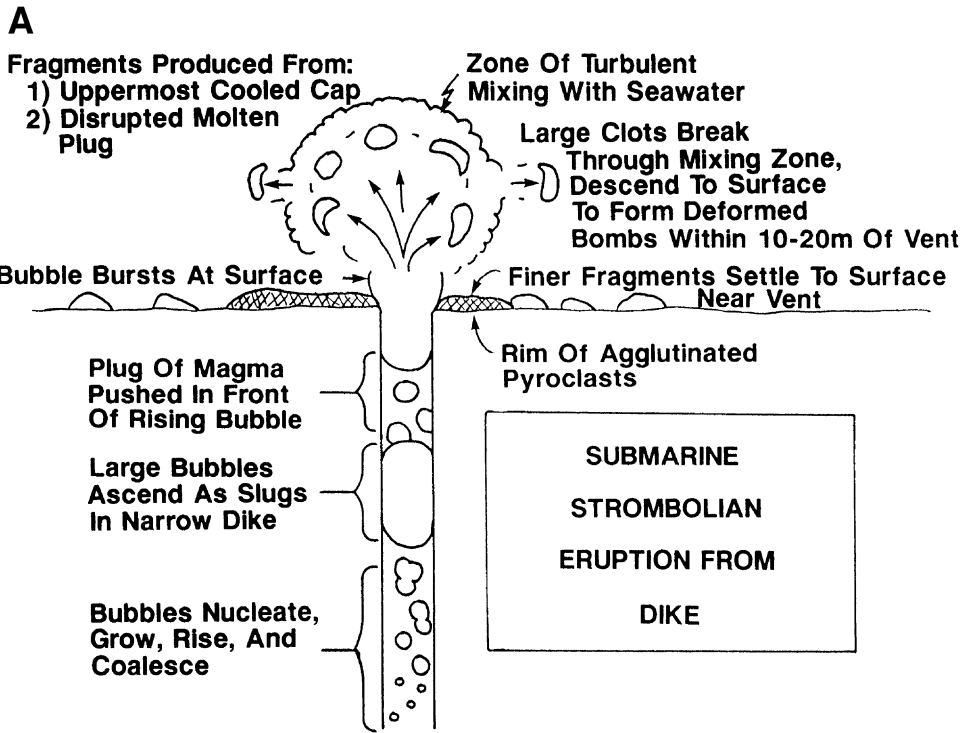


Fig. 5. Submarine strombolian eruptions. (A) Configuration of a vent. (B) Configuration of a lava pond. (C) Examples of subaerial eruptive products in the block to bomb size range (from [Macdonald, 1967](#)). Explanation: (A) bipolar fusiform bomb with lee side to top; (B) cross-section of bomb shown in (A); (C) unipolar fusiform bomb; (D) almond-shaped bomb; (E) cross-section of bomb shown in (D); (F) cross-section showing broad equatorial fin; (G) cylindrical ribbon bomb; (H) cross-section of bomb shown in (G); (K) cow-dung bomb; (J) cross-section of bomb shown in (K). (D) Example of a possible fragment derived from the top of a lava lake (from [Kokelaar, 1986](#)) and described in the text.

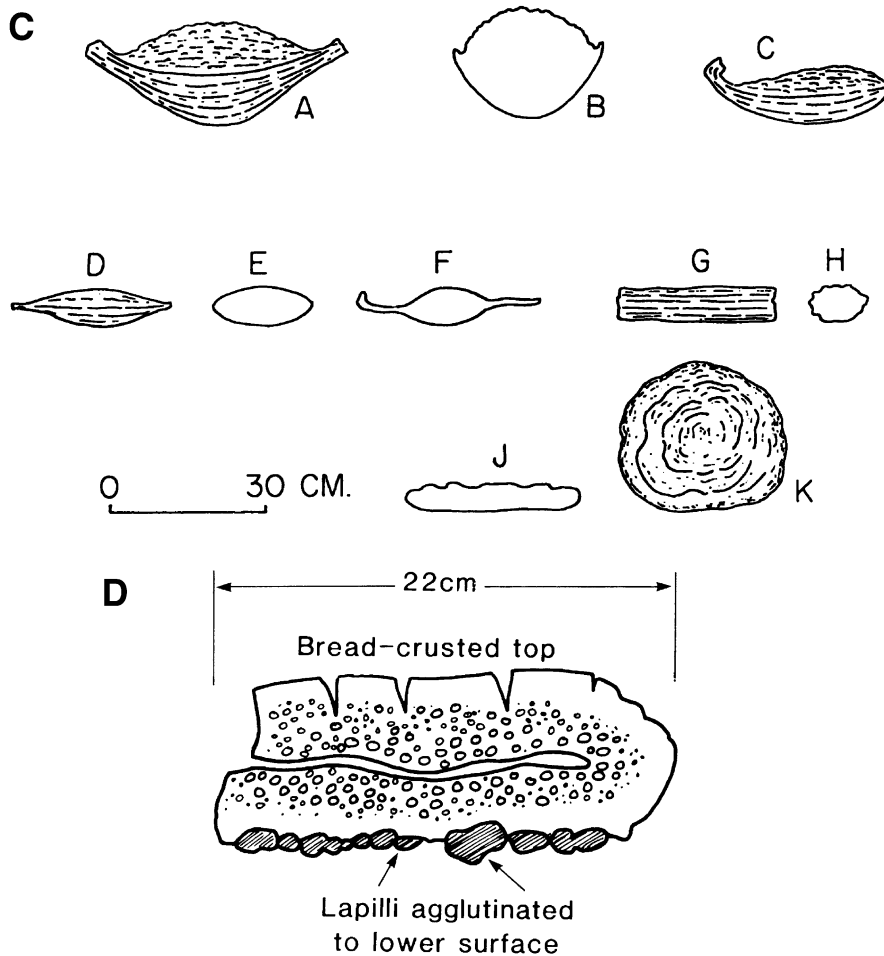


Fig. 5 (Continued).

flows and pillows rather than extensive lobate sheets (e.g. Head et al., 1996; Gregg and Fink, 1995). As the rise rate stabilized, and prior to the time that cooling closed off ascent, strombolian activity would occur as the gas bubble rise speed exceeded the magma rise speed. Disruption of magma would occur at the vent–water interface; the maximum bubble size for subaerial environments is about 5–10 m (Wilson and Head, 1981) and that of submarine environments under these conditions is about 1.5–2 m, being mainly controlled by the higher ambient pressure. Bubbles will rise more slowly (4–5 m/s) than in the subaerial case, and smaller bubbles mean that

there will be lower internal excess pressures (1–2 bar), and thus initial ejecta velocities will be small, but up to 20 m/s. As the bubbles burst (Fig. 5), fragments mingle with the surrounding water, and are cooled and drastically decelerated; fragments that might travel to maximum distances of 50–60 m in the subaerial environment are restricted to less than 10–20-m maximum distance in the submarine environment. Thus, water drag and deceleration of pyroclastic fragments is a key factor in both strombolian and hawaiian-style submarine eruptions and the resulting landforms. The maximum bubble sizes of 1–2 m mean that typical fragment sizes will be much smaller than this.

Table 6

Magma rise speed at great depth in the conduit system,  $u_s$ , and corresponding conduit width,  $W_s$ , which marks the boundary between strombolian activity and steady magma discharge

$\eta$ (Pa s)	Magma contains 0.4 wt% CO <sub>2</sub>		Magma contains 1.4 wt% CO <sub>2</sub>	
	$u_s$ (m/s)	$W_s$ (m)	$u_s$ (m/s)	$W_s$ (m)
30	0.5	0.30	2.0	0.60
100	0.2	0.35	0.8	0.69
300	0.1	0.42	0.4	0.85

Values are given as a function of magma viscosity,  $\eta$ , in basalts containing 0.4 and 1.4 wt% CO<sub>2</sub>. At higher magma rise speeds in wider conduits bubble coalescence is negligible and a steady discharge of vesicular magma (or, if the water depth above the vent is small enough, hawaiian-style explosive activity) will occur.

Expansion of the gas bubble just prior to bursting will tend to accelerate all particles to approximately the same initial velocity, but the greater inertia of the larger particles will mean that they will travel further, and one can anticipate blocks and bombs littering the surface beyond the edge of finer-grained deposits. Larger fragments (in the block, 64–256-mm, and bomb, > 256-mm, range) will probably be derived from the plug of magma pushed in front of the rising gas bubble (Fig. 5A), or from the cooled upper surface of a lava pond (Fig. 5B). The full spectrum of morphologies of bomb and block shapes might be anticipated (Fig. 5D), and the details of shapes, sizes, abundances and frequency distribution around specific vents are keys to the original eruption conditions. For example, a sample collected from a submarine eruption at Surtla (Fig. 5D; Kokelaar, 1986) could be similar to the types of features anticipated to be derived from the top of a lava pond; the cooled upper thermal boundary layer (chilled at the top, vesicular below) might be ripped apart by the expanding gas bubble (Fig. 5B), folded over in flight and, upon landing, still be hot enough to cause agglutination of lapilli onto its lower surface.

The pulses associated with the bursting of bubbles in strombolian events might provide the energy necessary to initiate contact-surface steam explosivity (e.g. Kokelaar, 1986, and see discus-

sion below). In this case, fragments might shatter, possibly repetitively, so that a series of shattering events might operate to reduce the average grain size until mm-sized fragments were formed; at that point, subsequent cooling would not generate sufficient steam to continue shattering by this process. Even with the extensive particle shattering that might occur during the contact-surface steam explosivity process, the volume density of particles is still very likely to be insufficient to make extensive density flows, and the particles would more likely settle to the surface to form a thin layer of cooled pyroclasts in the area immediately surrounding the vent (Fig. 5A,B).

Ejecta built up around a submarine strombolian vent would obviously be closer to the vent than in the subaerial case. The resulting cone would be no more than 20–40 m in maximum width, and would have a rim crest whose position was dictated by a combination of fragment size and velocity, and thus accumulation rate. Rim crests would probably be located at radii of less than about 10 m. Rim heights would depend on eruption duration, and on the basis of the simple cooling relations discussed above, might be limited to few meters. Initial strombolian events could build a low ring of agglutinated pyroclasts around the vent and thus provide the basis for accumulating a small lava pond or lake. The presence of a pond (Fig. 5B) could change the nature of the pyroclastic deposits; bubbles bursting in the cooler magma of the pond and disrupting a surface thermal boundary layer, the characteristics of which might vary as described above, would produce larger, cooler pyroclasts than in the earlier stages, and this should be reflected in the cone deposits. Strombolian activity is unlikely to be sufficiently vigorous and continuous under submarine conditions that it will lead to a distinctive mixing layer which undergoes collapse to produce gravity-driven pyroclastic flows. Lava flows associated with these types of cones, in addition to having a surface morphology consistent with very low effusion rates (predominantly pillows), should also be relatively depleted in vesicles. In summary, the types of deposits associated with strombolian activity should on average be dominated by relatively large clasts deposited near the

vent and often agglutinated and welded, cones with rim crest radii measuring a few meters, a lack of extensive pyroclastic flows, and associated lava flows with predominantly pillow textures. The role of smaller-scale pyroclastic fragments generated by contact-surface steam explosivity is at present unknown, but could clearly alter the size-frequency distribution of pyroclasts and resulting deposits.

### *2.7. Volatile content builds up in the top of dike leading to vulcanian eruptions*

In this case, which might occur following a period of strombolian or hawaiian activity, the top of the dike becomes sealed, and gas accumulates in the upper part of the dike (Figs. 2 and 6) leading to sufficient excess pressure that a vulcanian-type explosion takes place. In these events, the region around the top of the dike (consisting of country rock) will be broken into angular fragments, mixed with some juvenile material from the upper part of the dike, and ejected radially away from the point of the explosion (e.g. Head and Wilson, 1979). In the subaerial environment, fragments can be accelerated and transported to distances of kilometers (Fagents and Wilson, 1993), but in the submarine environment, the fragments will be rapidly decelerated by the surrounding seawater, drag forces being  $\sim 10^3$  times larger than subaerially, and will settle to the surface as a relatively chaotic mass of angular blocks, generally within just a few meters (less than 5 m) of the vent. There is no a priori reason to expect that a vulcanian event will be followed by extensive extrusive volcanism (because the ascent of material in the dike has already ceased and additional cooling has taken place as the volatiles have built up) and thus these types of events might be characterized by deposits of angular blocks of country rock without many subsequent lava flow deposits. Should effusion take place, it would more likely be at low rates and thus would be characterized by short pillow-lava flow dominated deposits, rather than extensive sheet flow deposits. A potential major variation on this theme is the possibility that the energy associated with the vulcanian explosion might provide the

threshold necessary to initiate contact-surface steam explosivity in the exposed magma in the top of the dike. In this case, the proximal blocky ejecta deposits might be veneered with hyaloclastic deposits. In addition, exposure of the top of the dike by the explosion might cause bulk interaction steam explosivity as seawater surged into contact with the exposed magma at the top of the dike. As soon as the water was converted to steam, however, the expanding wave would push water back out of the vent, suppressing further contact and permitting additional cooling to take place. This process seems self-limiting, but perhaps a few surges of cooling and quenching could take place to produce local pyroclastic deposits before equilibrium was reached.

## **3. Non-magmatic gas mechanisms for magma fragmentation and the production of hyaloclastites**

The range of magma–water interactions that might occur in subaqueous and emergent basaltic volcanism has been described by Kokelaar (1986) (Fig. 7). This includes the range of conditions that might result in the explosive release of magmatic volatiles that we have treated in detail above, as well as a variety of other mechanisms which we consider below and relate to magmatic gas release processes.

### *3.1. Cooling-contraction granulation*

In this mechanism, which can occur at any depth, magma comes into contact with water and cools by conductive heat transfer at its surface, thus developing a temperature gradient between the center and the surface of the fragment or feature (Figs. 7 and 8). Rapidly following the extrusion of lava underwater, the outer boundary layer becomes rigid and, when the interior cools, it will contract more than the outer layer can accommodate, so that cracking or granulation results. Among the deposits produced are dominantly sand- and granule-size grains which comprise a mixture of glassy globules commonly showing evidence of shattering in situ, and highly angular chunks and splinters of glass. These are



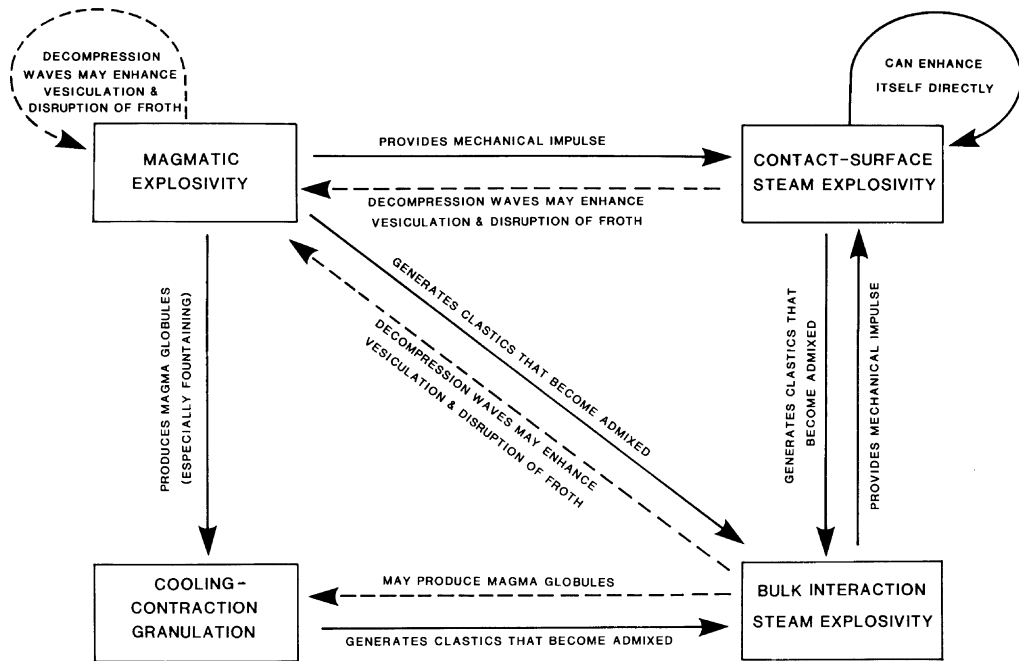


Fig. 7. Submarine clast-forming processes and possible enhancement mechanisms. From Kokelaar (1986).

blocky country rock ejecta and disrupted juvenile material forming volcanoclastics. If they form as submarine pseudocraters they might be relatively readily recognized as a series of small craters surrounded by ramparts of blocky ejecta and finer-grained pyroclastics. One might expect these features to be more abundant on sheet flows than on pillow basalts on the basis of the ability of sheet

flows to trap larger amounts of water over shorter periods of time. Features formed from intrusive events such as dike injection would appear very similar to those from vulcanian events described above. Differences might include variations in crater geometry and country rock size-frequency distribution based on the intrusion into a wet slurry in the bulk interaction steam explosivity example

**COOLING-CONTRACTION GRANULATION**

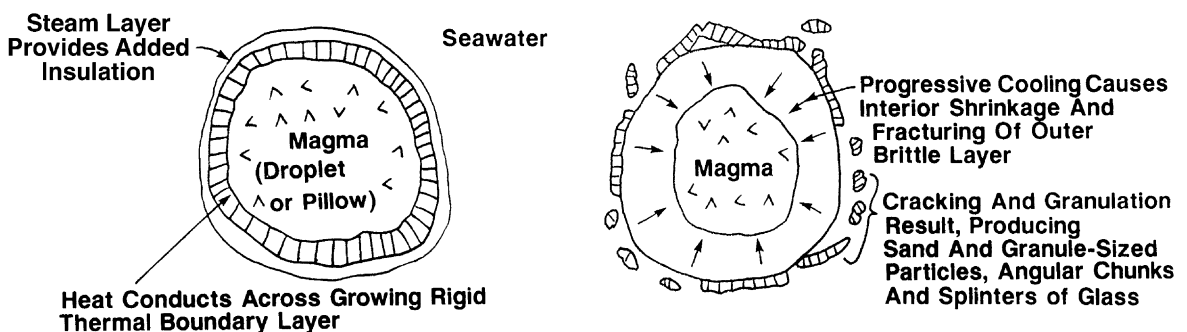


Fig. 8. Processes and environments of cooling-contraction granulation.

### BULK INTERACTION STEAM EXPLOSIVITY

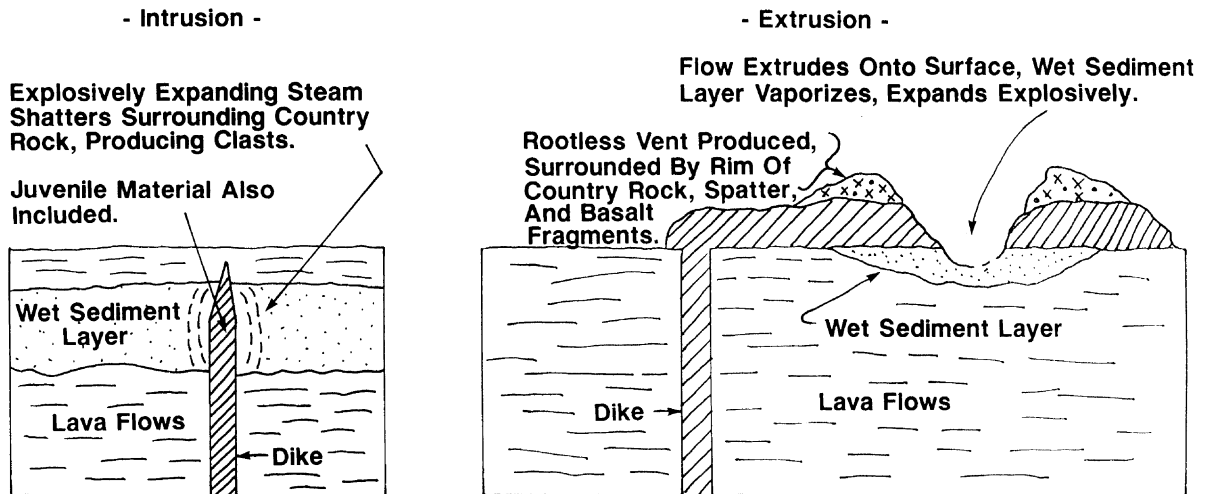


Fig. 9. Processes and environments of bulk interaction steam explosivity.

(e.g. shallower crater, smaller and less coherent fragments).

#### 3.3. Contact-surface steam explosivity

This mechanism, also known as fuel-coolant interaction, involves the explosive expansion and collapse of steam formed at magma-water contact surfaces (Figs. 1 and 7). It commonly requires initiation by vigorous impact between magma and water; although no certain depth limit is known, the likelihood of such explosivity decreases rapidly with increasing depth. The initial surface event is sufficiently vigorous to cause ongoing melt fragmentation, mixing with water, and heat transfer so that steam explosivity is capable of sustaining the interaction until the entire melt is fragmented. In such a sustained interaction, fragmentation and heat transfer occur extremely rapidly and they can be violently explosive; most of the melt is finely comminuted (a large proportion in the micron size range), and the explosion is extremely powerful (essentially a violent hydro-magmatic eruption) (Wohletz, 1983, 1986).

Two alternative models seem to account best for this process (Kokelaar, 1986; Wohletz, 1986). In one, the 'spontaneous nucleation model', su-

perheated water vaporizes instantaneously and produces homogeneous boiling. In the 'thermal detonation model', rapid vaporization occurs behind a propagating shock. Basically, when magma comes into contact with water, a thin film is formed along the contact surface by coalescing steam bubbles, and the film becomes unstable as it expands and collapses on a microsecond or millisecond scale. If the steam film oscillates vigorously, it may cause the magma to become finely fragmented and to mix turbulently with water. Explosions of this mixture can occur if either the water is superheated to its spontaneous vapor nucleation temperature (homogeneous boiling), or if the insulating steam film collapses or is disrupted by a pressure wave, causing further melt fragmentation, so that heat is rapidly exchanged and steam is instantly produced (thermal detonation). This interaction can be sustained since in either case the explosion can cause further melt fragmentation and turbulent mixing with water (Kokelaar, 1986; Fig. 7). Kokelaar (1986) cites the observations of decreasing amounts of clastic material with increasing depth to propose that contact-surface steam explosivity is limited by increasing hydrostatic pressure. For example, for thermal detonation, vapor expansion of sufficient

violence is needed to cause continued fragmentation and heat exchange capable of propagating the pressure wave and sustaining the interaction; increasing pressure with depth reduces the probability of achieving such propagation. Even at much lower pressures, however, experiments have shown (Wohletz, 1986) that pressure has stabilized vapor films and limited reactions. Thus, although triggers appear to work, they need to be increasingly vigorous at higher pressures and greater water depths, so that expansion aids the process and so that it does not become self-limiting.

In summary, increased confining pressure suppresses the process of contact-surface explosivity (Figs. 1 and 7) by limiting initial fragmentation and heat exchange during film boiling, by preventing spontaneous nucleation vaporization, and by requiring increasingly vigorous triggers to initiate interaction (Kokelaar, 1986). In the growth and vertical evolution of seamounts (Fig. 1), the transition from lava flows to volcanoclastic deposits does not necessarily require exsolution of magmatic volatiles, but can be accomplished in principle by contact-surface explosivity processes (Fig. 6). However, magmatic volatile explosivity is likely to be one of the principle causes of and initiators of contact-surface explosivity. Thus, great care should be taken to develop criteria to distinguish the characteristics of products and landforms produced by magmatic volatile explosivity processes (Figs. 2, 4 and 5) from those related to contact-surface explosivity processes.

#### **4. Summary of predictions of the style of emplacement of deposits and processes of formation of landforms**

On the basis of observations of deposits and landforms (e.g. Schmidt and Schmincke, 2000; Batiza and White, 2000) on a variety of seamounts (e.g. Smith and Batiza, 1989) and sea floor environments, and theoretical consideration of the ascent and eruption of basaltic magma (e.g. Head et al., 1996) under similar submarine conditions (Fig. 6), we now summarize a set of pre-

dictions (Table 7) that might be used to distinguish submarine effusive and explosive deposits produced under a variety of eruption conditions (Fig. 2). These predictions are designed to aid in the observation and interpretation of deep-sea landforms and their deposits, and to refine the theoretical treatments of the behavior of erupting magma under submarine conditions.

For magma compositions typical of spreading centers and their vicinity, the most likely circumstance in the depth ranges considered here is the quiet effusion of magma with minor gas exsolution, and the production of somewhat vesicular pillow lavas or sheet flows, depending on effusion rate (Head et al., 1996; Gregg and Fink, 1995). Eruption column heights would be measured in centimeters and would be insufficient to cause any magma disruption. Magma disruption from the exsolution of purely primary magmatic volatiles to produce hawaiian-style continuous fountaining (Figs. 2 and 4) would not be expected in these environments because primary magma volatile contents are considerably less than the several wt% required to cause disruption. Such eruptions might occur in some subduction zone environments where unusually high primary magma volatile contents are observed. Should such an eruption occur in the submarine environment at these depths (Fig. 1), one would anticipate a highly collimated gas-pyroclast column rising to a height of the order of a few meters, surrounded by a distinctive but narrow mixing zone which would collapse due to increased density to form an inner zone dominated by primary and rootless flows and agglutinated hot pyroclasts, and an outer zone or apron (meters to several tens of meters in extent) of pyroclastic density flows (Fig. 2). Due to the relatively high effusion rate, associated lava flows would tend to be sheet flows rather than pillow lavas.

The most likely mode of occurrence for pyroclastic deposits in the submarine environment and with mafic compositions is strombolian (Fig. 2), due to the artificial local buildup of volatiles in magma that has a low rise speed. In this case, magmatic gas collects by bubble coalescence, ascends, and reaches sufficient concentration that disruption of the magma occurs, producing local-

Table 7  
Predictions concerning characteristics and deposits for different eruption styles

	Lava flows	Vent characteristics	Cones	Pyroclastics deposits; agglutinates; blocks and bombs; hyaloclastite deposits	Density flows
(1) No gas exsolution:	No vesicles	?	–	–	–
(2) Gas exsolution, no magmatic disruption:	Vesicular	?	–	–	–
(3) Hawaiian-style fountaining: gas exsolution, magma disruption:	Vesicular sheet flows	Linear or circular pit	Meters to several tens of meters in diameter	Proximal welded deposits, distal fragmental and partly agglutinated	Surround vent and cone to tens of meters' radius
(4) Strombolian activity: magma volatile content insufficient of cause fragmentation; low magma rise speed causes artificial volatile enhancement:	Less vesicular, tend toward short pillow lavas	Crater	Rim crest < 10-m radius, agglutinated pyroclasts	Abundant blocks and bombs, finer fragments near vent	Density flows rare
(5) Vulcanian eruption: volatile content artificially builds up in top of dike:	May be ponds in crater	Explosion crater	Blocky cone	Blocks of country rock, minor hyaloclastites	–
(6) Enhanced hawaiian-style eruption: volatile content artificially builds up in magma reservoir forming foam:	Probably less vesicular	Crater	Cone broader and less steep	Deposits less agglutinated, more dispersed. No blocks or bombs	Density flows extensive, out to > 100-m radius

ized blocks, bombs, and pyroclastic deposits (Fig. 5). Because of the very low magma rise speeds, associated lava flows would be expected to be dominated by pillow lavas rather than sheet flows. These deposits can be distinguished from hawaiian eruption products and landforms by the abundance of blocks and bombs (Fig. 5C), the lack of extensive pyroclastic flow deposits (eruptive pulses are episodic and volumetrically small), and differences in the nature of associated lava flows (strombolian: pillow lavas, less vesicular; hawaiian: sheet flows, more vesicular).

Another possible mode of occurrence of pyroclastic deposits in the submarine environment is that resulting from vulcanian eruptions (Fig. 2). These deposits, being characterized by the dominance of angular blocks of country rocks deposited in the vicinity of a crater (Fig. 6), should be easily distinguished from strombolian and hawaiian eruptions.

Other modes of bulk-interaction steam explosivity (Fig. 7) may have similar characteristics (Fig. 9, left). The production of pseudocraters by the bulk-interaction steam explosivity mechanism (Fig. 9, right) should be distinguishable from strombolian eruptions by variations in the shape and size-frequency distribution of ejecta and its distribution around the vent (compare Figs. 5 and 9, right).

A special case of the hawaiian eruption style may occur if magmatic gas buildup occurs in a magma reservoir (Fig. 2). In this case, a layer of foam may build up at the top of the reservoir in sufficient concentrations to reach and even exceed the volatile contents necessary for disruption and hawaiian-style activity. In this case, the deposits and landforms are predicted to be somewhat different from those of a typical primary-magmatic-volatile-induced hawaiian eruption (Fig. 4). Spe-

cifically, typical pyroclast sizes might be smaller, pyroclasts might be dominated by broken bubble walls ('limu o Pele'), fountain heights may exceed those described in Fig. 4, cooling of descending pyroclasts would be more efficient, leading to different types of proximal deposits, and runout distances for density flows would be greater, potentially leading to surrounding pyroclastic deposits in the tens to hundreds of meters range. In addition, flows emerging after the consumption of the foam layer would tend to be very depleted in volatiles, and thus extremely poor in vesicles relative to typical flows associated with hawaiian-style eruptions in the primary magmatic gas case. Thus, sufficient differences appear to exist to distinguish between these two types of hawaiian eruption style (Table 5).

### 5. Relation of predictions to recent sea floor observations

Numerous sea floor exploration efforts have documented unusual pyroclastic and hyaloclastic deposits at a wide range of depths in the submarine environment. We now briefly examine a range of these observations in order to assess the applicability of the models developed in this contribution to the interpretation and observation of pyroclastic and hyaloclastic deposits.

Fouquet et al. (1998) reported on the discovery and documentation of extensive volcanoclastic deposits along the MAR axis (southwest of the Azores) that they suggested could be formed by deep-water explosive volcanic activity. They explored a series of three progressively deeper MAR segments, ranging from depths of ~400 to ~2000 m, each with different types of deposits. The shallowest segment (38°20'N; ~400 to ~930 m water depth) is about 45 km long, lacks a deep axial rift valley, and contains a circular 25-km diameter central volcano with a height of ~1200 m, which is bisected by a 2-km wide, 500-m deep axial graben. Exposed in the graben walls and on the floor is at least 400-m thickness of layered volcanoclastic ejecta, with individual layers ranging from a few mm to a few cm thick, consisting of sand and lapilli-sized clasts, and a

few m-thick poorly sorted lapilli layers. The intermediate depth segment (Menez Gwen; ~700 to ~1050 m water depth) is morphologically similar to the shallow one, with a central ~16-km diameter volcano having a height of ~700 m, bisected by a 2-km wide, 300-m deep axial graben. A 290-m thick volcanoclastic unit overlies a 60-m thick lava flow section containing flows up to 3 m thick. The deepest segment (Lucky Strike; 1570–~2000-m water depth) consists of a 15-km wide rift valley containing a central 12×8-km volcano with a 1-km wide central caldera; three dominantly scoriaceous breccia summit cones surround a restricted area of layered volcanoclastic deposits within the caldera. The central part of the caldera contains a lava lake with non-vesicular lobate and sheet flows. The volcanoclastic deposits are well-layered, but much thinner (< 10 m thick) and less extensive than those on the two shallower segments. The volcanic breccia deposits typical of the three summit cones (~1700 m) are dominated by massive fragmental units grading laterally into in situ breccias and coherent highly vesicular scoriaceous lava flows that locally form pillow lava.

Sea bottom reflectivity images enabled Fouquet et al. (1998) to extrapolate their submersible dive observations and showed that: (1) the volcanoclastic material is restricted to the center of the segments, forming most of the surface of the volcanic cones, (2) the area of the surface covered by volcanic deposits decreases with increasing depth (~67 to ~15 to ~2.8 km<sup>2</sup> for the three segments, respectively), (3) the deposits become thinner and less voluminous with depth, and (4) lava flows are the only deposits at the southern and northern ends of the three segments, whereas the volcanoclastics coexist with lava flows in the central part of the segment (suggesting to Fouquet et al. (1998) a relation to ridge segmentation).

The deposits themselves commonly consist of well-stratified ash layers, with normal and possibly reversed grading, very sharp bedding planes between lapilli and finer ash units, worm burrows at the tops of some beds, some intercalated mm-thick calcareous pelagic sediment, non-graded layers generally restricted to the very center of the segments, some layers with a matrix of pelagic

sediment, and decreasing total thickness as a function of increasing water depth (> 400, ~270 and < 10 m for the three segments). Thin sections showed that the predominant clast type is scoriaeous (30–50% vesicle volume) to pumiceous (50–80% vesicle volume) glass fragments, with highly vesicular glass fragments showing often extreme stretching, indicating acceleration and rapid deformation prior to and during quenching. No evidence of welding was observed. More common in the coarse-grained volcanoclastics are broken crystals and accidental lithic fragments. Geochemical analyses show that most of the glasses have a water concentration typical of N-MORB (< 0.4 wt%).

Fouquet et al. (1998) interpreted these characteristics to mean that the deposits were largely primary volcanoclastics from episodic and perhaps short-lived explosive eruptive events occurring repeatedly over long periods of time, with the non-graded layers representing proximal deposits. In addition they cited the following characteristics in support of their interpretation: (1) the layered nature is indicative of fallout deposits after magma fragmentation caused by the combined effects of expanding magmatic volatiles as well as hydro-magmatic processes involving seawater, (2) the lack of welding suggests that if any hot eruption facies were generated, they were of limited extent, and (3) the abundance of lithic clasts and broken crystals favors a magma–water explosive interaction such as that seen in maars, tuff cones or Surtsey-type hydromagmatic volcanism. They concluded that the bedded volcanoclastics resulted ‘from submarine explosions involving a combination of expansion of magmatic volatiles, bulk/surface steam explosivity of seawater and possibly thermal contraction fragmentation, which can occur at any depth, perhaps aided by a rapid extrusion rate’ (Fouquet et al., 1998). They concluded that their evidence suggested that explosive eruptions can occur and produce extensive deposits along mid-ocean ridges at considerably greater water depths (up to ~1700 m) than commonly believed. The preferential distribution of the deposits at the medial topographic highs of the three MAR segments suggested to them a preferential concentration of volatiles there.

The excellent descriptions and abundant evidence for submarine explosive volcanic eruptions documented by Fouquet et al. (1998) permit us to apply the theoretical models and predictions described above to these three examples, in order to develop further the interpretations of Fouquet et al. (1998), and to help distinguish among the roles of magmatic gas expansion, bulk/surface steam explosivity and thermal contraction fragmentation. We find that the deposits and relationships described at the two shallowest ridge segments are most consistent with magmatic gas exsolution, disruption and hawaiian-style pyroclastic fountaining. Evidence favoring hawaiian-style eruptions includes: (1) relatively wide dispersal, large thickness and volume of deposits, (2) relatively small grain size, (3) lack of sorting, (4) lack of welding, (5) elongation and stretching of fragments, and (6) presence and nature of layering.

We envision the following scenario for these events (Fig. 4A,B): juvenile volatile expansion leads to a sufficiently high gas bubble content to produce magmatic disruption and the rise of hawaiian-style plumes. Fragmentation associated with the gas expansion and disruption produces tephra composed of glassy vesicular bubble wall fragments, many of which have been stretched and elongated. Rapid mixing with seawater causes immediate quenching and the rising column becomes denser than adjacent seawater and begins to collapse. The outer margins of the collapsing column form a dense turbulent slurry which descends the flanks as a density current; some sorting, grading, and erosion of underlying deposits occurs. Multiple fountaining events cause successive flows and form additional layers; periods between such eruptions are characterized by calcareous sediment accumulation and biogenic reworking in the upper pyroclastic layers. This scenario is consistent with the characteristics of the deposits: (1) non-graded layers generally restricted to the very center of the segments (proximal density current deposits), (2) well-stratified ash layers, with normal and possibly reversed grading; very sharp bedding planes between lapilli and finer ash units (more distal density current deposits); the matrix of pelagic sediment seen in some layers could be eroded by the density cur-

rent from the underlying between-event calcareous sediment accumulation), and (3) worm burrows at the tops of some beds and some intercalated mm-thick calcareous pelagic sediment (layers deposited between eruption events).

In summary, hawaiian eruption style events appear to explain the vast majority of the observations without requiring a major role for bulk/surface steam explosivity and thermal contraction fragmentation, although such processes will inevitably accompany submarine magmatic and explosive eruptions. If these deposits are produced by hawaiian eruptions, is enhanced primary magmatic gas content or artificial buildup in the summit of the reservoir required (Fig. 2)? Volatile contents cited by Fouquet et al. (1998) (typical of N-MORB, <0.4 wt%) would require no enhancements to cause disruptions at depths of less than ~500 m. At depths typical of the deeper parts of the shallow segment and the intermediate depth segment, some additional gas buildup is required for basalts of this composition. We favor the artificial buildup of gas in foams at the top of the magma reservoir for the shallow and intermediate depth cases for the following reasons: (1) the locations of these extensive deposits are at the center and topographic summit of a ridge segment, where the central magma reservoir is predicted to reside on the basis of the geometry of dike emplacement (e.g. see Head et al., 1996 and references therein), and (2) the buildup of foam in the reservoir will lead to much more vigorous pyroclastic fountains which we interpret to be more consistent with the thickness, large lateral extent (out to 1 km) and volumes of the observed deposits.

Fouquet et al. (1998) note that the landforms and deposits of the deepest segment (Lucky Strike) differ significantly from those of the two shallower segments. These pyroclastic deposits are characterized by smaller volumes, less extensive dispersal, and coarser-grained clasts. The cones at the summit of the central edifice are characterized by volcanic breccia that they interpreted as being produced by autobrecciation, downslope re-sedimentation, and/or cooling-contraction granulation. We interpret these pyroclastic deposits to be the distal products of strombolian eruptions

(Fig. 5A,B), with artificial gas buildup being caused by relatively high rise rate of bubbles compared with magma, and the coalescence and growth of these bubbles leading to the disruption of the magma surface and the ejection of pyroclasts to the vicinity of the vent. Adjacent to these deposits within the caldera is a lava lake with non-vesicular lobate and sheet flows. The non-vesicularity of these deposits is consistent with their degassing during a period of strombolian activity and their subsequent eruption.

In summary, we concur with the interpretation of Fouquet et al. (1998) that these deposits are of pyroclastic origin and we further suggest that hawaiian-style eruptions dominate the two shallowest MAR segments, whereas strombolian-style eruptions dominate the deepest segment. We do not discount the possibility that hydrothermally circulating water contributed to the explosivity of these eruptions, but stress that the small vesicle sizes and relatively uniform distributions of vesicles in the bulk of the clasts imply that if external water was incorporated into these magmas, it must have been absorbed by solution at the depth of the magma reservoirs to ensure its uniform distribution in the magma.

Clague et al. (2002c) described submarine spatter and volcanic bombs in alkalic basalts from Kaua'i and submarine spatter of tholeiitic composition from Kilauea's submarine east rift zone eruption, and interpreted them to be indicative of submarine strombolian eruptions. Abundant samples of bubble-wall fragments ('limu o Pele') collected along the submarine rift zone of Kilauea and the Gorda Ridge axis are interpreted as mildly explosive strombolian eruption events.

From alkalic vents on the south side of Kaua'i, Clague et al. (2002c) described highly vesicular spatter, ribbon spatter, breadcrust bombs, a spindle bomb, and a large block of agglutinated spatter. These are precisely the kinds of features that are predicted by the model calculations (Fig. 5A–D), and we concur with Clague et al. (2002c) in their interpretation of these as representative of strombolian-style eruptions. Enhanced volatile content can be attributed to both the higher volatile abundance of alkalic basalts and the concentration of volatiles by bubble coalescence.

‘Limu o Pele’ were originally described by [Hon et al. \(1988\)](#) in an environment where lava entered the ocean and produced bubbles in the lava due to incorporation of seawater into the stream of lava and its expansion to steam. Following this interpretation, [Clague et al. \(2000\)](#) attributed ‘limu o Pele’ found on the Puna Ridge at about 2200 m depth, on the Lo’ihi Seamount at 1150–1950 m depth, and on Seamount 6 at 1600–2000 m depth, to be due to the expansion of seawater during boiling following its contact with lava. However, the discovery of ‘limu o Pele’ from volcanic cones in the North Arch lava field at 4160 m depth, i.e. a depth significantly greater than the critical point of seawater ([Clague et al., 2002a](#)), and from the Gorda Ridge (~2800 m depth; [Clague et al., 2002c](#)), led to the reinterpretation of these deposits as being derived from a separated magmatic gas phase during strombolian eruptions ([Clague et al., 2002c](#)). [Clague et al. \(2002c\)](#) further suggest that such strombolian activity may be very common along the entire mid-ocean ridge magmatic system, that seismic reflection profiles may in part be detecting the presence of coalesced gas layers or volcanic foams in the upper ridge reservoirs that are feeding the strombolian eruptions, and that event plumes previously interpreted to be hydrothermal discharges may also be composed of a significant component of magmatic gas.

We concur with the interpretation of [Clague et al. \(2002c\)](#) that ‘limu o Pele’ could be produced by strombolian activity. However, the presence of ‘limu o Pele’ in itself does not necessarily distinguish strombolian eruptions from hawaiian eruptions. Thus, additional information is required to distinguish adequately between these two mechanisms, particularly since the buildup of foams at the top of magma reservoirs can lead to hawaiian eruptions at significant depths. For example, the relative proportions of vesicles might be one indicator, with few to no vesicles favoring strombolian eruptions of more degassed magma, and more abundant vesicles favoring hawaiian-style eruptions. These types of observations, together with the relative abundance of ‘limu o Pele’ versus spatter, might help to distinguish eruption types.

Furthermore, the presence of magmatic foams

feeding hawaiian eruptions could make even more dramatic two of the factors cited by [Clague et al. \(2002c\)](#): (1) the possible presence of strong reflectors at the top of magma reservoirs would be significantly enhanced due to magmatic foam buildup, and (2) event plumes consisting of a significant magmatic gas component could be even more extensive if they were part of a hawaiian-style eruption that transferred the gas directly into the ocean. The source of the event plume in a submarine hawaiian eruption would not be the jet itself (because it collapses; [Fig. 4B](#)), but could be the more widespread sea floor pyroclastic deposit, producing an upwelling comparable to a subaerial co-ignimbrite plume.

The summit of Lo’ihi Seamount lies at about 1200 m depth and exploration there has revealed a variety of pyroclastic deposits interpreted by [Clague et al. \(2002b\)](#) to be evidence for phreatic, phreatomagmatic, hawaiian and strombolian eruptions. Extensive units including spatter, bombs and bubble wall fragments (‘limu o Pele’) are interpreted as evidence of strombolian activity. The presence of scoriaceous fragments and Pele’s hair is cited as evidence of hawaiian eruptive activity. The presence of cored bombs, coarse-grained basalt fragments, hydrothermally altered basalt and glass fragments, and hydrothermal stockwork fragments are interpreted to represent phreatic and possibly phreatomagmatic eruption styles, perhaps related to caldera or pit crater formation. We concur with these interpretations but note that ‘limu o Pele’ is also very likely to be associated with hawaiian-style submarine eruptions, as discussed above, and that vulcanian eruption products ([Fig. 6](#)) may be difficult to distinguish from deposits of phreatic, phreatomagmatic and bulk interaction steam explosivity ([Fig. 9](#)) eruption styles.

Particles attributed by [Clague et al. \(2002b\)](#) to hawaiian eruptions are mostly alkalic basalts, while those attributed to other eruption types are tholeiitic and transitional basalts. The volatile content of the Lo’ihi alkalic basalts ([Clague et al., 2002c](#)) (~1.5 wt% CO<sub>2</sub>) is insufficient to cause simple hawaiian disruption ([Fig. 2](#), example 3), according to the calculations we presented earlier ([Table 3](#)), and thus magmatic gas enhancement

through the development of magmatic foams at the tops of subsurface reservoirs seems to be required (Fig. 2, example 6). This situation seems very likely because of the high likelihood of the presence of a large magma reservoir beneath the Lo'ihi summit.

Deep sea drilling has also revealed that deep submarine pyroclastic eruptions may be more common than previously thought. For example, hole 396B, which was drilled approximately 150 km east of the MAR (22°59.14'N, 43°30.90'W), encountered (from top to bottom) 225 m of sediment, 175 m of pillow basalts, and 90 m of loose, sand-size, glassy basaltic debris (hyaloclastite) with some associated broken-pillow breccia (Schmincke et al., 1978). That the clastic unit was primary and not produced during the drilling process was indicated by bedding in some of the volcanoclastics, a high ratio of sideromelane to crystalline basalt (up to 60%), and the high degree of brecciation and vesiculation of overlying and underlying pillow breccias. Furthermore, according to Schmincke et al. (1978) the near-synchronicity of eruptions and the glass production process, and the lack of extensive transportation of the fragmental material from the site of brecciation, were suggested by: (1) the high ratio of glass to crystalline basalt, and (2) the relative chemical homogeneity of the glass in the bedded volcanoclastite. The units formed ~13 Ma ago, and due to the fact that eruptions occurred at depths estimated to be >3000 m, Schmincke et al. (1978) concluded that the confining pressures implied by these depths precluded explosive volcanic activity due to primary magmatic volatile exsolution and disruption, as well as sea-water vaporization. Instead, the major processes of formation of the sideromelane shards was attributed to 'spalling of pillow rinds to produce "spallation" shards [...] but implosion of pillows and granulation of lava may also have occurred' (Schmincke et al., 1978, p. 341). According to the authors, the process of fragmentation of tachylite shards is unknown. Furthermore, Schmincke et al. (1978) note that the sideromelane in the deposit is extremely fresh, suggesting that the clastic unit was sealed off from percolating seawater since its formation about 13 Ma ago.

On the basis of the theoretical treatments and predictions described earlier in this paper, we believe that the characteristics of the bedded clastic unit outlined by Schmincke et al. (1978) may be alternatively explained in the context of primary magmatic volatile exsolution and disruption, such as that characteristic of hawaiian and strombolian eruption styles. Given the plausibility of hawaiian eruptions even at these great depths due to the buildup of magmatic gas foams in the top of a reservoir (Fig. 2, example 6), the characteristics of the deposit might be explained as a hawaiian-style eruption of such a magmatic foam for the following reasons.

(1) Vesicle-rich overlying lava flows suggest that volatiles are exsolving during magma rise, storage and eruption in this environment.

(2) The very close association of the flows and the bedded clastics suggests formation in the same environment.

(3) The absence of alteration (palagonitization) suggests that the glass shards have not been in contact with seawater and thus that they underwent 'rapid sedimentation' preserving them in a dry environment for 13 Ma; such an environment may have been the intermediate portions of the mixing zone of a hawaiian eruption plume (Fig. 4A,B) dominated by CO<sub>2</sub> gas, where pyroclastic-glass and CO<sub>2</sub>-rich density flows descended rapidly from the plume and deposited material proximally and buried it rapidly before significant seawater mixing and penetration had taken place.

(4) The presence of indurated volcanoclastite and the absence of crystalline basalt fragments in it suggest that this material may have been the result of emplacement in the warmer more proximal parts of density flows produced by the collapsing column (Fig. 4B). These would be dominated by glass fragments and are more likely to be welded.

(5) The presence of loose and unindurated volcanoclastites and the common presence of crystalline basalt fragments in the loose material suggests that these deposits may have been derived from the outer part of the eruption plume mixing zone, where mixing with seawater is more thorough and collapse and resulting density currents produce unwelded deposits which incorporate the

substrate (the basalt fragments). The presence of foraminifera and bedding in these deposits further supports the emplacement in such an environment.

On the basis of these observations, and the thickness of the deposits, we believe that the deposits can be interpreted in the context of a hawaiian-style eruption resulting from the release of a magmatic foam built up at the MAR magma reservoir. While strombolian activity may have also occurred, the volume of the deposits as well as their apparent rapid and flow-like emplacement, favors a major role for hawaiian eruptions. The thickness of the deposits suggests that the vent was in relatively close proximity and that there was more than one eruptive phase. Although spalling of pillow rinds and implosion of pillows and granulation of lava may also have occurred (e.g. Schmincke et al., 1978), hawaiian eruptions seem to be a more likely dominant process.

## 6. Critical observations for interpretations and further assessment of models

Continued sea floor exploration is essential in order to test the models outlined here and to provide new observations to refine and modify them. Important observations that need to be made in order to understand further the modes and styles of submarine eruptions include the following:

(1) *Vent characteristics.* What is the nature of the vent? Does it appear constructional, or created from an explosion? Does it appear rootless and superposed on a flow or is it the source of flows and other deposits? What is the width of the vent? What is the shape of the vent (elongate, circular, deep, shallow, etc.)?

(2) *Cones.* What is the diameter of the cone, its rim height, its shape, and the radius to the rim crest? What are the surface deposits on the cone and how do they vary as a function of distance from the vent or rim crest? Is any stratigraphy exposed in the cone?

(3) *Blocks and bombs.* Are these primary magmatic (e.g. cow-dung bombs) or angular blocks of ejected country rock? What is their size-frequency

distribution, and how does this change as a function of distance from the vent? What is their morphology (see Fig. 5C)? What is the detailed structure and morphology of bomb surfaces? What is the radial range of the largest fragment and what is its size and shape? Are blocks and bombs welded to the surface or do they have agglutinated undersides?

(4) *Volcaniclastic deposits.* What is the distribution of these deposits relative to vents? What is their thickness as a function of range? How does this vary as a function of azimuth? What is the nature of these deposits? What is the vesicle size distribution? Do they contain non-magmatic particles (e.g. fragmental bedrock or incorporated sediment)? What is the shape and relative abundance of different types of pyroclastic particles in volcaniclastics? Is 'limu o Pele' present, in what abundance, and what is its importance relative to other pyroclastic fragments? Is Pele's hair present? Is there evidence for graded bedding? What is the relationship of hyaloclastites to lava flows? What are the key associations? Are blocks and bombs observed in association with proximal and distal pyroclastic deposits? Are finer-grained (cm-sized) particles littered on top of pyroclastic deposits? If so, what is their vesicularity?

(5) *Lava flows.* What is the form and surface texture of lava flows (e.g. pillows, sheet flows, etc.)? Where do they occur in relation to other deposits in both time (superposed, covered) and space (e.g. marginal to pyroclastic flows, capping the vent around pyroclastic flow deposits, etc.)? What are the general associations of each flow type (e.g. pillow lavas and blocks and bombs, sheet flows and agglutinated cone deposits, etc.)? What is the vesicularity of rocks associated with each flow type?

## 7. Summary and implications

The detailed models of the ascent and eruption of magma in the submarine environment that are developed here show that significant pyroclastic activity can occur even at depths in excess of 3000 m and that a wide range of pyroclastic deposits should be anticipated. Mid-ocean ridge

magma reservoirs may be environments favoring the buildup of magmatic foams and their rapid release, producing hawaiian-style eruptions and associated pyroclastics. On the basis of the nature of ridge segmentation and magma reservoir formation and evolution, such foam buildups would be favored at topographic highs in the middle of ridge segments. Furthermore, the episodic nature of dike emplacement at divergent plate boundaries also produces conditions in which magma rise rates in dikes are often low, and bubble coalescence and magmatic gas rise rates are relatively high, leading to magma disruption at the top of the dike and strombolian-style eruptive activity. The latter stages of development of volcanic edifices (seamounts) formed in submarine environments are also excellent candidates for a wide range of submarine pyroclastic activity. This is due not just to the effects of decreasing water depth, but also to: (1) the presence of a summit magma reservoir, which favors the buildup of magmatic foams (enhancing hawaiian-style activity) and episodic dike emplacement (which favors strombolian-style eruptions), and (2) the common occurrence of alkalic basalts, the CO<sub>2</sub> contents of which favor submarine explosive eruptions at depths greater than tholeiitic basalts. Pyroclastic deposits resulting from vulcanian eruptions (characterized by the dominance of angular blocks of country rocks deposited in the vicinity of a crater), should be easily distinguishable from those due to strombolian and hawaiian eruptions, but will be more difficult to distinguish from products of phreatic or phreatomagmatic eruptions styles. Bulk-interaction steam explosivity and contact-surface steam explosivity contribute to volcanoclastic (hyaloclastite) formation in these submarine environments.

The presence of previous submarine explosive eruptive activity can be detected through the analysis of the resulting deposits, as outlined here. In addition, instrumentation of candidate sites of submarine explosive activity might include one or more of the following approaches.

(1) *Active seismic studies.* Although magmatic foam layers may be relatively thin (tens of meters), the location of volatile concentrations at the top of magma reservoirs, both on mid-ocean

ridge summits and seamount summits, may be detectable by seismic methods, as suggested by Clague et al. (2002c). Furthermore, if volcanoclastic deposits are common in some parts of the upper crust, they may complicate the interpretation of Layer 2a (e.g. Schmincke et al., 1978, where a 90-m thick layer is described from a DSDP drill hole); alternatively, high resolution active seismic techniques might be used to map the extent of such deposits.

(2) *Passive seismic studies.* Submarine explosive eruptions will be accompanied by seismic activity. Seismic activity associated with different explosive eruption styles will differ from that typical of dike emplacement (e.g. laterally migrating, episodic swarm activity; Fox et al., 1995) and is predicted to have the following characteristics.

- for hawaiian eruptions: intermediate intensity sustained activity from a central source lasting hours to several days;
- for strombolian eruptions: lower level intermittent activity from a central source or sources;
- for vulcanian eruptions: high intensity spike-like activity from a central source.

(3) *Gas and thermal plume detection.* A range of gas release styles is predicted from submarine pyroclastic eruptions, and as pointed out by Clague et al. (2002c), some of the event plumes that are associated with seismic swarms (e.g. Embley and Chadwick, 1994; Fox et al., 1995) could be related to magmatic gas eruption as well as large-scale hydrothermal discharge (e.g. Baker, 1998). Our treatment shows that the most efficient transfer of magmatic gas into seawater above dikes or vents occurs in strombolian eruptions, where large gas bubbles are segregated from the magma and erupted directly into the seawater. The H<sub>2</sub>O component of these bubbles will condense and the CO<sub>2</sub> component will dissolve into the water to produce narrow, CO<sub>2</sub>-rich, thermal plumes rising directly toward the surface. Magmatic gas released during submarine hawaiian-style activity is predicted to be closely linked to hot pyroclasts that mix with seawater at the margins of the eruptive column and become dense enough to collapse and produce marginal density currents that spread laterally for distances of up to a kilometer. Gas release from these types of events will thus

largely occur in the terminal phases of emplacement and will therefore be more dispersed in seawater, more diffuse in area, and occur over a longer time period than the strombolian case. Such differences in predicted behavior suggest that careful monitoring programs may be able to distinguish hydrothermal discharges from both submarine explosive eruptions and the slow diffusion of gas from intruded dike tops.

Finally, the submarine environment on Earth is similar in many ways to the surface environment on Venus, where a thick CO<sub>2</sub> atmosphere produces surface pressures equivalent to depths of about 1000 m on the Earth's sea floor, sufficient to suppresses juvenile gas exsolution such that magmatic disruption and pyroclastic activity is not favored under normal conditions (e.g. Head and Wilson, 1986, 1992). In previous treatments, strombolian activity seemed to be the most likely candidate for explosive eruptions on Venus (Head and Wilson, 1986), but the results of the present analysis suggest that the buildup of magmatic foams at the top of reservoirs on Venus (e.g. Pavri et al., 1992) may also favor the local occurrence of hawaiian-style eruptions.

### Acknowledgements

We gratefully acknowledge helpful discussions with Rodey Batiza and David Clague. Thanks are extended to Leonid Dmitriev for productive discussions and bringing to our attention the presence of glassy sands and volcanoclastics recovered from the MAR during the *Glomar Challenger* DSDP drilling and dredging from the R/V *Akademik Boris Petrov*. Special thanks are extended to Rodey Batiza for arranging for the participation of J.W.H. in two cruises (R/V *Atlantis II*, October 1995; R/V *Ka'imikai-o-Kanaloa*, October 1998) and associated submersible dives to study seamounts and submarine pyroclastic eruptions. Special thanks are extended to the pilots and support crews of the submersibles *Alvin* and *Pisces IV* with particular thanks to *Pisces IV* pilot Terry Kerby for his interest and dedication to scientific exploration. Thanks are further extended to Richard Fiske and David Clague for detailed re-

views that resulted in a significant improvement of the manuscript. Financial support is gratefully acknowledged from PPARC (Grant PPA/G/S/2000/00521 to L.W.) and the NASA Planetary Geology and Geophysics Program (NAG5-10690 to J.W.H.).

### References

- Baker, E.T., 1998. Patterns of event and chronic hydrothermal venting following a magmatic intrusion: New perspectives from the 1996 Gorda Ridge eruption. *Deep-Sea Res. II* 45, 2599–2618.
- Batiza, R., White, J.D.L., 2000. Submarine lavas and hyaloclastite. In: Sigurdsson, H., Houghton, B., McNutt, S.R., Rymer, H., Stix, J. (Eds.), *Encyclopedia of Volcanoes*. Academic Press, San Diego, CA, pp. 361–381.
- Batiza, R., Fornari, D.J., Vanko, D.A., Lonsdale, P., 1984. Craters, calderas and hyaloclastites on young Pacific seamounts. *J. Geophys. Res.* 89, 8371–8390.
- Binard, N., Hekinian, R., Cheminee, J.L., Stoffers, P., 1992. Styles of eruptive activity on interplate volcanoes in the Society and Austral hot spot regions: Bathymetry, petrology, and submersible observations. *J. Geophys. Res.* 97, 13999–14015.
- Blake, S., 1981. Volcanism and the dynamics of open magma chambers. *Nature* 289, 783–785.
- Bonatti, E., Harrison, C.G.A., 1988. Eruption styles of basalt in oceanic spreading ridges and seamounts: Effect of magma temperature and viscosity. *J. Geophys. Res.* 93, 2967–2980.
- Bottinga, Y., Javoy, M., 1990. Mid-ocean ridge basalt degassing: Bubble nucleation. *J. Geophys. Res.* 95, 5125–5131.
- Bruce, P.M., Huppert, H.E., 1989. Thermal control of basaltic fissure eruptions. *Nature* 342, 665–667.
- Buck, W.R., Delaney, P.T., Karson, J.A., Lagabrielle, Y. (Eds.), 1998. *Faulting and Magmatism at Mid-Ocean Ridges*. Geophysical Monograph 106. American Geophysical Union, Washington, DC.
- Cashman, K.V., Fiske, R.S., 1991. Fallout of pyroclastic debris from submarine volcanic eruptions. *Science* 253, 275–280.
- Cashman, K.V., Sturtevant, B., Papale, P., Navon, O., 2000. Magmatic fragmentation. In: Sigurdsson, H., Houghton, B., McNutt, S.R., Rymer, H., Stix, J. (Eds.), *Encyclopedia of Volcanoes*. Academic Press, San Diego, CA, pp. 421–430.
- Clague, D.A., Davis, A.S., Bischoff, J.L., Dixon, H.E., Geyer, R., 2000. Lava bubble-wall fragments formed by submarine hydrovolcanic explosions on Loihi Seamount and Kilauea Volcano. *Bull. Volcanol.* 61, 437–449.
- Clague, D.A., Uto, K., Satake, K., Davis, A.S., 2002a. Eruption style and flow emplacement in the submarine North Arch Volcanic Field, Hawaii. In: *Hawaiian Volcanoes: Deep Underwater Perspectives*. Am. Geophysical Monograph 128, American Geophysical Union, Washington, DC, pp. 65–84.

- Clague, D.A., Batiza, R., Head, J.W., Davis, A.S., 2002b. Phreatic, Phreatomagmatic, Hawaiian, and Strombolian Eruption Products at the Summit of Loihi Seamount, Hawaii. *Am. Geophys. Union Spec. Publ. on Submarine Volcanism*, American Geophysical Union, Washington, DC, in press.
- Clague, D.A., Davis, A.S., Dixon, J.E., 2002c. Submarine strombolian eruptions in Hawaii and along the Gorda Mid-ocean Ridge. In: *Explosive Subaqueous Volcanism*. *Am. Geophysical Monograph*, American Geophysical Union, Washington, DC, in press.
- Davis, A.S., Clague, D.A., 1998. Changes in the hydrothermal system at Loihi Seamount after the formation of Pelee's Pit in 1996. *Geology* 26, 399–402.
- Devine, J.D., Sigurdsson, H., 1995. Petrology and eruption styles of Kick'em-Jenny submarine volcano, Lesser Antilles island arc. *J. Volcanol. Geotherm. Res.* 69, 35–58.
- Dixon, J.E., 1997. Degassing of alkalic basalts. *Am. Mineral.* 82, 368–378.
- Dixon, J.E., Clague, D.A., 2001. Volatiles in basaltic glasses from Loihi Seamount, Hawaii: Evidence for a relatively dry plume component. *J. Petrol.* 42, 627–654.
- Dixon, J.E., Stolper, E.M., 1995. An experimental study of water and carbon dioxide solubilities in mid-ocean ridge basaltic liquids, Part II. Applications to degassing. *J. Petrol.* 36, 1633–1646.
- Dixon, J.E., Clague, D.A., Stolper, E.M., 1991. Degassing history of water, sulfur, and carbon in submarine lavas from Kilauea Volcano, Hawaii. *J. Geol.* 99, 371–394.
- Dixon, J.E., Stolper, E.M., Holloway, J.R., 1995. An experimental study of water and carbon dioxide solubilities in mid ocean ridge basaltic liquids, 1. Calibration and solubility models. *J. Petrol.* 36, 1607–1631.
- Dixon, J.E., Clague, D.A., Wallace, P., Poreda, R., 1997. Volatiles in alkalic basalts from the North Arch volcanic field, Hawaii: Extensive degassing of deep submarine-erupted alkalic series lavas. *J. Petrol.* 38, 911–939.
- Embley, R.W., Chadwick, W.W., 1994. Volcanic and hydrothermal processes associated with a recent phase of seafloor spreading at the northern Cleft segment: Juan de Fuca Ridge. *J. Geophys. Res.* 99, 4741–4760.
- Fagents, S.A., Wilson, L., 1993. Explosive volcanic eruptions – VII. The ranges of pyroclasts ejected in transient volcanic explosions. *Geophys. J. Int.* 113, 359–370.
- Fisher, R.V., Schmincke, H.-U., 1984. *Pyroclastic Rocks*. Springer, Berlin.
- Fiske, R.S., Cashman, K.V., Shibatas, A., Watanabe, K., 1998. Tephra dispersal from Myojinsho, Japan, during its shallow submarine eruption of 1952–1953. *Bull. Volcanol.* 59, 262–275.
- Fiske, R.S., Naka, J., Iizasa, K., Yuasa, M., Klaus, A., 2001. Submarine silicic caldera at the front of the Izu–Bonin arc, Japan: Voluminous seafloor eruptions of rhyolite pumice. *Geol. Soc. Am. Bull.* 113, 813–824.
- Fornari, D.J., Perfit, M.R., Allan, J.F., Batiza, R., 1988. Small-scale heterogeneities in depleted mantle source: Near-ridge seamount lava geochemistry and implications for mid-ocean-ridge magmatic processes. *Nature* 331, 511–513.
- Fouquet, Y., Eissen, J.-P., Ondreas, H., Barriga, F., Batiza, R., Danyushevsky, L., 1998. Extensive volcanoclastic deposits at the Mid-Atlantic Ridge axis: Results of deep-water basaltic explosive volcanic activity. *Terra Nova* 10, 280–286.
- Fox, C.G., Radford, W.E., Dziak, R.P., Lau, T.-K., Matsumoto, H., Schreiner, A.E., 1995. Acoustic detection of a seafloor spreading episode on the Juan de Fuca Ridge using military hydrophone arrays. *Geophys. Res. Lett.* 101, 281–295.
- Gerlach, T.M., 1991. Midocean ridge popping rocks – Implications for degassing at ridge crests – Comment. *Earth Planet. Sci. Lett.* 105, 566–567.
- Gill, J., Torssander, P., Lapierre, H., Taylor, R., Kaiho, K., Koyama, M., Kusakabe, M., Aitchison, J., Cisowski, S., Dadey, K., Fujioka, K., Klaus, A., Lovell, M., Marsaglia, K., Pezard, P., Taylor, B., Tazaki, K., 1990. Explosive deep water basalt in the Sumisu backarc rift. *Science* 248, 1214–1217.
- Greeley, R., Fagents, S.A., 2001. Icelandic pseudocraters as analogs to some volcanic cones on Mars. *J. Geophys. Res.* 106, 20527–20546.
- Gregg, T.K.P., Fink, J.H., 1995. Quantification of submarine lava-flow morphology through analog experiments. *Geology* 23, 73–76.
- Harris, D.M., 1981. The concentration of CO<sub>2</sub> in submarine tholeiitic basalts. *J. Geol.* 89, 689–701.
- Head, J.W., Wilson, L., 1979. Alphonsus-type dark-halo craters: Morphology, morphometry and eruption conditions. *Proc. Lunar Planet. Sci. Conf.* 10, 2861–2897.
- Head, J.W., Wilson, L., 1986. Volcanic processes and landforms on Venus: Theory, predictions, and observations. *J. Geophys. Res.* 91, 9407–9446.
- Head, J.W., Wilson, L., 1987. Lava fountain heights at Pu'u O'o, Kilauea, Hawaii: Indicators of amount and variations of exsolved magma volatiles. *J. Geophys. Res.* 92, 13715–13719.
- Head, J.W., Wilson, L., 1989. Basaltic explosive eruptions: Influence of gas-release patterns and volume fluxes on near-vent dynamic morphology, and the formation of subsequent pyroclastic deposits (cinder cones, spatter cones, rootless flows, lava ponds, and lava flows). *J. Volcanol. Geotherm. Res.* 37, 261–271.
- Head, J.W., Wilson, L., 1992. Magma reservoirs and neutral buoyancy zones on Venus: Implications for the formation and evolution of volcanic landforms. *J. Geophys. Res.* 97, 3877–3903.
- Head, J.W., Wilson, L., 2002. Mars: Geologic setting of magma/H<sub>2</sub>O interactions. In: Smellie, J.E., Chapman, M.G. (Eds.), *Volcano-Ice Interactions on Earth and Mars*. Geological Society of London Spec. Publ., London, in press.
- Head, J.W., Wilson, L., Smith, D.K., 1996. Mid-ocean ridge eruptive vent morphology and structure: Evidence for dike widths, eruption rates, and evolution of eruptions and axial volcanic ridges. *J. Geophys. Res.* 101, 28265–28280.
- Heikinian, R., Bideau, D., Stoffers, P., Cheminee, J., Muhe,

- R., Puteanus, D., Binard, N., 1991. Submarine intraplate volcanism in the South Pacific: Geologic setting and petrology of the Society and Austral region. *J. Geophys. Res.* 96, 2109–2138.
- Hon, K., Heliker, C.C., Kjargaard, J.I., 1988. Limu o Pele: A new kind of hydroclastic tephra from Kilauea Volcano, Hawaii. *Geol. Soc. Am. Abst. Prog.* 20, A112–A113.
- Hunns, S.R., McPhie, J., 1999. Pumiceous peperite in a submarine volcanic succession at Mount Chalmers, Queensland, Australia. *J. Volcanol. Geotherm. Res.* 88, 239–254.
- Javoy, M., Pineau, F., 1991. The volatiles record of a 'popping' rock from the Mid-Atlantic Ridge at 14°N: Chemical and isotopic composition of gas trapped in the vesicles. *Earth Planet. Sci. Letts.* 107, 598–611.
- Kano, K., 1998. A shallow-marine alkali-basalt tuff cone in the Middle Miocene Jinzai Formation, Izumo, SW Japan. *J. Volcanol. Geotherm. Res.* 87, 173–191.
- Keating, B., Fryer, P., Batiza, R., Boehlert, W. (Editors), 1987. *Seamounts, Islands and Atolls*. Geophysical Monograph 43, American Geophysical Union, Washington, DC.
- Kent, A.J., Clague, D.A., Honda, M., Stolper, E.M., Hutchison, I.D., Norman, M.D., 1999. Widespread assimilation of a seawater-derived component at Loihi Seamount, Hawaii. *Geochim. Cosmochim. Acta* 63, 2749–2761.
- Keszthelyi, L.P., McEwen, A.S., Thordarson, T., 2000. Terrestrial analogs and thermal models for martian flood lavas. *J. Geophys. Res.* 105, 15027–15049.
- Kokelaar, P., 1986. Magma–water interactions in subaqueous and emergent basaltic volcanics. *Bull. Volcanol.* 48, 275–290.
- Kokelaar, P., Busby, C., 1992. Subaqueous explosive eruption and welding of pyroclastic deposits. *Science* 257, 196–201.
- Lonsdale, P., Batiza, R., 1980. Hyaloclastite and lava flows on young seamounts examined with a submersible. *Geol. Soc. Am. Bull.* 91, 545–554.
- Macdonald, G.A., 1967. Basalts: The Poldervaart Treatise on Rocks of Basaltic Composition. In: Hess, H.H., Poldervaart, A. (Eds.), Wiley, New York, pp. 1–482.
- Macdonald, K.C., 1998. Linkages between faulting, volcanism, hydrothermal activity and segmentation on fast spreading centers. In: Buck, W.R., Delaney, P.T., Karson, J.A., Lagabriele, Y. (Eds.), *Faulting and Magmatism at Mid-Ocean Ridges*. Geophysical Monograph 106, American Geophysical Union, Washington, DC, pp. 27–58.
- Maicher, D., White, J.D.L., 2001. The formation of deep-sea limu o Pele. *Bull. Volcanol.* 63, 482–496.
- Maicher, D., White, J.D.L., Batiza, R., 2000. Sheet hyaloclastite: Density current deposits of quench and bubble-burst fragments from thin glassy sheet lava flows, Seamount 6, Eastern Pacific Ocean. *Mar. Geol.* 171, 75–94.
- Mangan, M.T., Cashman, K.V., Newman, S., 1995. Vesiculation of basaltic magma during eruption. *Geology* 31, 157–160.
- Oshima, S., Tsuchide, M., Kato, S., Watanabe, K., Kudo, K., Ohsaka, J., 1991. Birth of a submarine volcano Teisi Knoll. *J. Phys. Earth* 39, 1–19.
- Parfitt, E.A., Wilson, L., 1995. Explosive volcanic eruptions – IX. The transition between Hawaiian-style lava fountaining and Strombolian explosive activity. *Geophys. J. Int.* 121, 226–232.
- Parfitt, E.A., Wilson, L., 1999. A Plinian treatment of fallout from Hawaiian lava fountains. *J. Volcanol. Geotherm. Res.* 88, 67–75.
- Parfitt, E.A., Wilson, L., Head, J.W., 1993. Basaltic magma reservoirs: Factors controlling their rupture characteristics and evolution. *J. Volcanol. Geotherm. Res.* 55, 1–14.
- Pavri, B., Head, J.W., Klose, K.B., Wilson, L., 1992. Steep-sided domes on Venus: Characteristics, geologic setting, and eruption conditions from Magellan data. *J. Geophys. Res.* 97, 13445–13478.
- Perfit, M.R., Chadwick, Jr., W.W., 1998. Magmatism at mid-ocean ridges: Constraints from volcanological and geochemical investigations. In: Buck, W.R., Delaney, P.T., Karson, J.A., Lagabriele, Y. (Eds.), *Faulting and Magmatism at Mid-Ocean Ridges*. Geophysical Monograph 106, American Geophysical Union, Washington, DC, pp. 59–115.
- Pineau, F., Javoy, M., 1994. Strong degassing at ridge crests: The behaviour of dissolved carbon and water in basalt glasses at 14°N, Mid-Atlantic Ridge. *Earth Planet. Sci. Letts.* 123, 179–198.
- Prandtl, L., 1949. *The Essentials of Fluid Dynamics*. Blackie, Edinburgh.
- Rittmann, A., 1960. *Vulkane und ihre Tätigkeit*. Enke, Stuttgart, 335 pp.
- Ryan, M.P., Blevins, J.Y.K., Okamura, A.T., Koyanagi, R.Y., 1983. Magma reservoir subsidence mechanics: Theoretical summary and application to Kilauea Volcano, Hawaii. *J. Geophys. Res.* 88, 4147–4181.
- Schmidt, R., Schmincke, H.-U., 2000. Seamounts and island building. In: Sigurdsson, H., Houghton, B., McNutt, S.R., Rymer, H., Stix, J. (Eds.), *Encyclopedia of Volcanoes*. Academic Press, San Diego, CA, pp. 383–402.
- Schmincke, H.-U., Robinson, P.T., Ohnmacht, W., Flower, M. F.J., 1978. Basaltic hyaloclastites from hole 396B, DSDP Leg 46. In: Dmitriev, L., Heirtzler, J. et al. (Eds.), *Initial Reports of the Deep Sea Drilling Project 46*, US Government Printing Office, Washington, DC, pp. 341–348.
- Smith, T.L., Batiza, R., 1989. New field and laboratory evidence for the origin of hyaloclastite flows on seamount summits. *Bull. Volcanol.* 51, 96–114.
- Sparks, R.S.J., 1978. The dynamics of bubble formation and growth in magmas: A review and analysis. *J. Volcanol. Geotherm. Res.* 3, 1–37.
- Squyres, S.W., Wilhelms, D.E., Moosman, A.C., 1987. Large-scale volcano-ground ice interaction on Mars. *Icarus* 70, 385–408.
- Thorarinsson, S., 1953. The crater groups in Iceland. *Bull. Volcanol.* 14, 3–44.
- UKCPS (United Kingdom Committee on the Properties of Steam), 1970. *UK Steam Tables 1970*. Edward Arnold, London.
- Vergnolle, S., Jaupart, C., 1990. Dynamics of degassing at Kilauea Volcano, Hawaii. *J. Geophys. Res.* 95, 2793–2809.
- Wallace, P., Anderson, A.T., 2000. Volatiles in magmas. In:

- Sigurdsson, H., Houghton, B., McNutt, S.R., Rymer, H., Stix, J. (Eds.), *Encyclopedia of Volcanoes*. Academic Press, San Diego, CA, pp. 149–170.
- Wessell, P., Lyons, S., 1997. Distribution of large Pacific seamounts from Geosat/ERS-1: Implications for the history of intraplate volcanism. *J. Geophys. Res.* 102, 22459–22475.
- White, J.D.L., 1996. Pre-emergent construction of a lacustrine basaltic volcano, Pahvant Butte, Utah (USA). *Bull. Volcanol.* 58, 249–262.
- White, J.D.L., 2000. Subaqueous eruption-fed density currents and their deposits. *Precamb. Res.* 26, 87–109.
- Wilson, L., 1980. Relationships between pressure, volatile content and ejecta velocity in three types of volcanic explosion. *J. Volcanol. Geotherm. Res.* 8, 297–313.
- Wilson, L., Head, J.W., 1981. Ascent and eruption of basaltic magma on the Earth and Moon. *J. Geophys. Res.* 86, 2971–3001.
- Wilson, L., Head, J.W., 1988. Nature of local magma storage zones and geometry of conduit systems below basaltic eruption sites: Pu'u 'O'o, Kilauea East Rift, Hawaii, example. *J. Geophys. Res.* 93, 14785–14792.
- Wilson, L., Head, J.W., 1994. Mars: Review and analysis of volcanic eruption theory and relationships to observed landforms. *Rev. Geophys.* 32, 221–263.
- Wilson, L., Heslop, S.E., 1990. Clast sizes in terrestrial and martian ignimbrite lag deposits. *J. Geophys. Res.* 95, 17309–17314.
- Wohletz, K.H., 1983. Mechanisms of hydrovolcanic pyroclast formation: Grain-size, scanning electron microscopy, and experimental results. *J. Volcanol. Geotherm. Res.* 17, 31–63.
- Wohletz, K.H., 1986. Explosive magma–water interactions: Thermodynamics, explosion mechanisms, and field studies. *Bull. Volcanol.* 48, 245–264.
- Wohletz, K.H., McQueen, R.G., 1984. Experimental studies of hydromagmatic volcanism. In: *Explosive Volcanism: Inception, Evolution, and Hazards, Studies in Geophysics*. National Academy Press, Washington, DC, pp. 158–169.
- Wolfe, E.W., Neal, C.A., Banks, N.G., Duggan, T.J., 1988. Geologic observations and chronology of eruptive events. In: Wolfe, E.W. (Ed.), *The Puu Oo Eruption of Kilauea Volcano, Hawaii: Episodes 1 through 20, January 3, 1983, through June 8, 1984*. US Geological Survey Professional Paper 1463, US Geological Survey, Reston, VA.
- Wright, I.C., 1996. Volcaniclastic processes on modern submarine arc stratovolcanoes: Sidescan and photographic evidence from the Rumble IV and V volcanoes, southern Kermadec Arc (SW Pacific). *Mar. Geol.* 136, 21–39.
- Wright, I.C., 1999. Southern Kermadec submarine caldera arc volcanoes (SW Pacific): Caldera formation by effusive and pyroclastic eruption. *Mar. Geol.* 161, 207–227.
- Zimanowski, B., Frohlich, G., Lorenz, V., 1991. Quantitative experiments on phreatomagmatic explosions. *J. Volcanol. Geotherm. Res.* 48, 341–358.